

# Nuclear-Cytoplasmic Localization of Acetyl Coenzyme A Synthetase-1 in the Rat Brain

Prasanth S. Ariyannur,<sup>1</sup> John R. Moffett,<sup>1</sup> Chikkathur N. Madhavarao,<sup>1</sup> Peethambaran Arun,<sup>1</sup> Nisha Vishnu,<sup>1</sup> David M. Jacobowitz,<sup>1</sup> William C. Hallows,<sup>2</sup> John M. Denu,<sup>2</sup> and Aryan M.A. Nambodiri<sup>1\*</sup>

<sup>1</sup>Department of Anatomy, Physiology and Genetics, Molecular and Cell Biology Program and Neuroscience Program, Uniformed Services University of the Health Sciences, Bethesda, Maryland 20814

<sup>2</sup>Department of Biomolecular Chemistry, School of Medicine and Public Health, University of Wisconsin, Madison, Wisconsin 53706

## ABSTRACT

Acetyl coenzyme A synthetase-1 (AceCS1) catalyzes the synthesis of acetyl coenzyme A from acetate and coenzyme A and is thought to play diverse roles ranging from fatty acid synthesis to gene regulation. By using an affinity-purified antibody generated against an 18-mer peptide sequence of AceCS1 and a polyclonal antibody directed against recombinant AceCS1 protein, we examined the expression of AceCS1 in the rat brain. AceCS1 immunoreactivity in the adult rat brain was present predominantly in cell nuclei, with only light to moderate cytoplasmic staining in some neurons, axons, and oligodendrocytes. Some nonneuronal cell nuclei were very strongly immunoreactive, including those of some oligodendrocytes, whereas neuronal nuclei ranged from unstained to moderately stained. Both antibodies stained some neuronal cell bodies and axons, especially in the hindbrain. AceCS1 immunoreactivity was stronger

and more widespread in the brains of 18-day-old rats than in adults, with increased expression in oligodendrocytes and neurons, including cortical pyramidal cells. Expression of AceCS1 was substantially up-regulated in neurons throughout the brain after controlled cortical impact injury. The strong AceCS1 expression observed in the nuclei of CNS cells during brain development and after injury is consistent with a role in nuclear histone acetylation and therefore the regulation of chromatin structure and gene expression. The cytoplasmic staining observed in some oligodendrocytes, especially during postnatal brain development, suggests an additional role in CNS lipid synthesis and myelination. Neuronal and axonal localization implicates AceCS1 in cytoplasmic acetylation reactions in some neurons. *J. Comp. Neurol.* 518:2952–2977, 2010.

© 2010 Wiley-Liss, Inc.

**INDEXING TERMS:** immunohistochemistry; acetate; histone acetylation; gene expression; lipid synthesis; traumatic brain injury; N-acetylaspartate; oligodendrocytes; neurons

Acetyl coenzyme A synthetase-1, AMP-forming type (AceCS1; EC 6.2.1.1), also known as acetate-coenzyme A ligase, is an evolutionarily conserved enzyme thought to function in various anabolic and catabolic pathways (Ingram-Smith and Smith, 2007), including lipid synthesis (Goldberg and Brunengraber, 1980; Luong et al., 2000). AceCS1 was originally identified from rat liver (Imesch and Rous, 1984) and is involved in production of acetyl coenzyme A from free acetate for, among other metabolic functions, the synthesis of fatty acids and sterols. Because of its involvement in lipid synthesis, this enzyme has until recently been thought to be expressed predominantly in the cytoplasm of cells. The activity of AceCS1 varies according to the nutritional status of the animal (Kornacker and Lowenstein, 1965; Woodnutt and Parker, 1978), and its mRNA expression is regulated by sterol

regulatory element-binding proteins (Luong et al., 2000; Sone et al., 2002). In contrast, the mitochondrial form of the enzyme, AceCS2, identified from ox heart, has a putative mitochondrial targeting sequence, is found mainly in extra hepatic tissues, and is involved in the synthesis of acetyl coenzyme A for energy production via the

Additional Supporting Information may be found in the online version of this article.

Grant sponsor: National Institutes of Health; Grant number: RO1 NS39387 (to A.M.A.N.); Grant sponsor: National Institute of Mental Health; Grant number: ZO-1-MH-00388-31 LCS (to D.M.J.).

\*CORRESPONDENCE TO: Aryan M.A. Nambodiri, Department of Anatomy, Physiology and Genetics, and Neuroscience Program, Uniformed Services University of the Health Sciences, 4301 Jones Bridge Rd., Bethesda, MD 20814. E-mail: anambodiri@usuhs.mil

Received February 19, 2009; Revised February 16, 2010; Accepted February 24, 2010

DOI 10.1002/cne.22373

Published online March 23, 2010 in Wiley InterScience (www.interscience.wiley.com)

© 2010 Wiley-Liss, Inc.

tricarboxylic acid cycle under ketogenic conditions (Fujino et al., 2001; Hallows et al., 2006; Sakakibara et al., 2009). The two enzymes have an approximate 50% peptide sequence homology. Northern blot analysis of AceCS mRNA in adult rat tissues has shown that AceCS1 is highly expressed in the liver and kidney, but only moderately in the brain and spleen, with very low expression in the heart. The mitochondrial form is highly expressed in the heart and less in the liver and kidney (Fujino et al., 2001). An in situ hybridization study of AceCS1 mRNA in the rat embryo showed expression of this enzyme in the brain, spinal cord, kidney, and liver during development (Loikkanen et al., 2002). The activities of AceCS1 and AceCS2 are regulated posttranslationally by acetylation, which inactivates both forms. NAD<sup>+</sup>-dependent deacetylases, known as *sirtuins*, act to reactivate the two enzymes (Starai et al., 2002). Distinct sirtuins are responsible for activating the cytoplasmic and mitochondrial forms of AceCS, with SIRT1 acting to deacetylate AceCS1 and SIRT3 acting to deacetylate AceCS2 (Hallows et al., 2006; Schwer and Verdin, 2008).

Recent studies have clarified some of the uncertainties over the functions served by the two forms of AceCS in eukaryotes. In yeast cells, the homolog of AceCS1 (designated *Acs2p* in yeast) has been found to be a nuclear-cytosolic enzyme that is involved in histone acetylation and gene regulation (Falcon et al., 2010; Takahashi et al., 2006). Histone acetyltransferases (HATs) acetylate histone proteins, resulting in disassembly of histone-DNA complexes, permitting gene transcription. Acetyl coenzyme A provides the acetate that HAT enzymes utilize to acetylate chromatin, highlighting the importance of the various metabolic sources of acetyl coenzyme A in chromatin remodeling. Two enzymes have been implicated as possible sources of acetyl coenzyme A for histone acetylation reactions, namely, AceCS1 and ATP citrate lyase (ACL). With several mammalian cell lines in culture, Wellen and colleagues (2009) used small inhibitory RNA to silence activity of either AceCS1 or ACL and found that both enzymes provided substrate for histone acetylation reactions. In the mammalian cell lines that they used, ACL contributed more acetyl coenzyme A for histone acetylation than did AceCS1.

In AceCS2 knockout mice, plasma acetate levels are markedly elevated, acetate oxidation rates are diminished, and the animals exhibit greatly reduced thermogenesis from brown adipose tissue (Sakakibara et al., 2009). In addition, ATP levels in the skeletal muscle of AceCS2<sup>-/-</sup> mice were profoundly reduced after 48 hours of fasting. This suggests that one primary role for AceCS2 is to provide energy under ketogenic conditions such as fasting and raises the intriguing question of the origin of the plasma acetate in these mice. Both liver and gut are

reported to release free acetate into the bloodstream when plasma acetate levels are low (Skutches et al., 1979).

Acetyl coenzyme A is a key cellular metabolite at the juncture between energy derivation and energy storage, depending on the nutritional state of the organism. When levels of nutrients such as glucose are low, most acetyl coenzyme A enters the citric acid cycle in mitochondria for oxidation and ATP production. When glucose levels are high, acetyl coenzyme A is converted to citrate in the citric acid cycle and exported to the cytoplasm for other metabolic functions, including the synthesis of fatty acids and sterols. Many protein functions are regulated by acetylation and deacetylation reactions (Spange et al., 2009), and, as part of this regulatory process, protein deacetylase enzymes generate free acetate, which cannot be further metabolized until it is converted into acetyl coenzyme A by one of the acetyl coenzyme A synthases. Very few studies have attempted to localize AceCS protein expression in various tissues. To our knowledge, there have been no studies on the immunohistochemical localization of AceCS1 protein expression in the mammalian brain. Here we provide a cellular expression profile of the nuclear-cytosolic form of AceCS in the adult rat brain, as well as in developing and injured rat brain, with two newly generated anti-AceCS1 antibodies.

## MATERIALS AND METHODS

### Generation of anti-AceCS1 peptide antibody

To identify cells expressing AceCS1, we selected a 19-mer N terminal sequence (MGLPEERRKSGSGSRAREE) from the published mouse AceCS1 sequence for immunizations (NCBI Genbank accession ID *AF216873*). This sequence was selected based on its low sequence similarity with other proteins in the database and maximal sequence dissimilarity from the mitochondrial acetyl coenzyme A synthetase enzyme. AceCS1 and AceCS2 perform the same enzymatic function and therefore have the same enzyme classification number (EC 6.2.1.1); however, they are the products of two distinct genes (NCBI *AF216873* and *AB046742*), which have minimal nucleotide sequence homology and only about a 50% amino acid sequence homology. Two amino acids at the N-terminus of the selected sequence (M and G) were deleted and a cysteine residue was added, making it an 18-mer peptide sequence. The peptide sequence was synthesized in the core facility of the Uniformed Services University of the Health Sciences. For antibody production, this newly synthesized peptide was conjugated to carrier proteins through the N-terminal cysteine residue in the sequence. Conjugation of the peptide to the carrier proteins was done using the cysteine cross-linker reagent sulfo-SMCC

[sulfosuccinimidyl 4-(N-maleimidomethyl)cyclohexane-1-carboxylate] according to the procedure given by the supplier (Pierce, Rockford, IL). To avoid production of antibodies that recognize the carrier proteins, we rotated the carrier proteins between keyhole limpet hemocyanin and bovine thyroglobulin for the first two immunizations. For the third round of immunization, the free peptide was mixed with colloidal gold particles (50 nm diameter) and used for immunizations. It has been reported that use of colloidal gold as a carrier increases titer values and facilitates the production of highly specific antibodies even against small molecules, such as glutamate and GABA (Pow and Crook, 1993). With this method, we generated a high-titer anti-AceCS1 sera, with the most specific antibodies coming from the third immunization and bleed using colloidal gold as the carrier.

### Affinity purification of the anti-peptide AceCS1 polyclonal antisera

Polyclonal sera against the 18-mer sequence were purified on an affinity column prepared with the peptide sequence used for immunizations. Affinity columns were prepared by coupling the N-terminus cysteine of the 18-mer AceCS1 peptide to the column matrix by the iodoacetamide method according to the manufacturer's protocol (SulfoLink Immobilization Kit for Peptides; Pierce). A 2-ml affinity column was equilibrated with phosphate-buffered saline (PBS; 10 mM phosphate, 150 mM NaCl, pH 7.2) with 2% normal goat serum (NGS), and 100  $\mu$ l antiserum (third immunization) was diluted to 5 ml with PBS plus 2% NGS. The solution was loaded onto the column and was circulated slowly in a loop through the column using a peristaltic pump (2 ml/minute) at room temperature for 16 hours. Unbound antiserum was drained, and the column was washed sequentially with 8 ml PBS, followed by 8 ml PBS containing 0.5 M NaCl. The antibodies were eluted with 8 ml of 2 M  $MgCl_2$  dissolved in PBS, and the eluate was collected in a tube containing 600  $\mu$ l NGS. The eluates were dialyzed immediately against PBS (200 times volume, one buffer change, 3 hours each) to remove  $MgCl_2$ , and the purified antibody preparation was stored with 0.1% sodium azide at 4°C.

### Immunoprecipitation

A 10% rat brain homogenate was prepared in PBS (pH 7.2) containing 1 mM CHAPS, 1 mM DTT, and protease inhibitor cocktail (Sigma-Aldrich, St. Louis, MO). Equal volumes (100  $\mu$ l) of homogenate and affinity-purified anti-peptide antibody (diluted 1:5 with IP buffer containing 100 mM Tris-HCl and 150 mM NaCl with 1 mM DTT) were incubated overnight at 4°C on a rocking platform. The antibody control consisted of 1% bovine serum albumin.

Protein G agarose (Pierce) was washed twice, and a 50% slurry was made with the IP buffer. One hundred microliters of the protein G agarose slurry was added to the antibody-brain homogenate mixture and incubated at room temperature for 2 hours with constant agitation. The slurry was then centrifuged at 2,500g for 3 minutes to remove the protein G agarose beads. The supernatants were used for AceCS1 activity assays.

### Acetyl coenzyme A synthetase assay

An AceCS1 colorimetric assay was done by using pyrophosphate detection as described previously (Kuang et al., 2007), with minor modifications. Assay conditions included 250  $\mu$ l solution containing 50 mM Tris-HCl, 10 mM sodium acetate, 1 mM magnesium chloride, 10 mM DTT, 4 mM ATP, and 0.15 mM CoA. Equal volumes of supernatant samples were added and kept at 37°C for 20 minutes. Assays were performed in duplicates. The reactions were stopped and the samples centrifuged at 15,000g for 6 minutes at 4°C. Aliquots of 95  $\mu$ l for each assay were added separately to Eppendorf tubes, followed by the addition of 12.5  $\mu$ l 2-mercaptoethanol (0.5 M), 2.5% molybdate reagent, and 5  $\mu$ l Eikonogen reagent (see Kuang et al., 2007). After equilibrating at room temperature for 10 minutes, the absorbance at 580 nm was determined with a Beckman DU spectrophotometer (Beckman DU 530 UV/VIS).

### Generation of polyclonal antibodies to full-length AceCS1 protein

Recombinant AceCS1 was produced and purified as previously described (Hallows et al., 2006). Rabbits were immunized with purified recombinant AceCS1 protein and were given additional immunizations three more times at 28-day intervals. Polyclonal antibodies from the final bleed were used for Western blotting and immunohistochemistry.

### SDS-PAGE and Western blot

SDS-PAGE and Western blotting were done as previously described (Madhavarao et al., 2004), with modifications. Briefly, SDS-PAGE was performed in 10% precast Tris-glycine gels (Invitrogen, Carlsbad, CA) loaded with equal protein concentrations from a 10% rat brain homogenate preparation. Protein concentrations were determined by Bio-Rad's DC protein assay (Bio-Rad, Hercules, CA), based on the method of Lowry. The gels were blotted onto a PVDF membrane (Sigma) for 90 minutes at a 25 V constant setting. The membranes were then blocked with 5% normal goat serum (Sigma) in PBS/Tween-20 (0.01%) buffer for 1 hour, followed by incubation with the varying concentrations of affinity-purified AceCS1 primary

**TABLE 1.**  
Primary Antibodies Used in the Current Study

Antigen	Immunogen	Details	Dilutions <sup>1</sup>
Acetyl-coenzyme A synthase 1 (AceCS1 peptide)	19-mer N-terminal sequence of AceCS1: (MGLPEERRKSGSGSRAREE)	Polyclonal antibody raised in rabbits: affinity purified	1:1,300 IP 1:500 IF
Acetyl-coenzyme A synthase 1 (AceCS1 protein)	Purified recombinant AceCS1 protein (protein purification described by Hallows, Lee, and Denu, 2006)	Polyclonal antibody raised in rabbits	1:5,000 IP 1:1,000 IF
Glial fibrillary acidic protein (GFAP)	Enriched bovine glial filaments	Rat monoclonal, protein G purified (Zymed, Invitrogen, No. 13-0300)	1:100 IF
CC1	Recombinant protein consisting of amino acids 1–226 of APC (adenomatous polyposis coli)	Mouse monoclonal (Calbiochem No. OP80)	100 IF

<sup>1</sup>IP, immunoperoxidase; IF, immunofluorescence.

antibody (1:500) overnight in a cold room. The membranes were washed three times (10 minutes each) with PBS/Tween-20 and treated with the goat anti-rabbit secondary antibodies (1:1,000; KPL Inc., Gaithersburg, MD) for 1 hour. After washing (three times for 10 minutes each) with the PBS/Tween-20, the membranes were developed for visualization using Sigma Fast DAB Reagent tablets.

### Immunofluorescence histochemistry

Ten adult male and four adult female Wistar rats weighing between 200 and 250 g (Taconic Inc, Rockville, MD) were used for this study. The animals were kept on a normal day–night light cycle and were given food and water ad libitum. Perfusions were done between 10 AM and 2 PM. Animals were deeply anesthetized with pentobarbital and perfused transcardially with 400 ml of 4% freshly depolymerized paraformaldehyde (Alfa Aesar, Ward Hill, MA) in deionized water (pH 7.2) by using a peristaltic pump at a flow rate of approximately 60–80 ml/minute. Brains and cervical spinal cords were carefully dissected and postfixed in 4% paraformaldehyde for approximately 1 hour. The tissues were cryoprotected by sequential passage through 10%, 20%, and 30% sucrose in water for 1 day each. Tissues were kept in 30% sucrose with 0.1% sodium azide at 4°C until use. The brains were rapidly frozen, and 10–20- $\mu$ m coronal sections were cut in a cryostat set at a temperature of –20°C. Some sections were collected directly on treated slides, whereas others were processed by the free-floating method. Sections collected on treated slides were stored at –70°C until further use for fluorescence immunohistochemistry. Brain and spinal cord sections in PBS were stored at 4°C until further use. Peroxidase and fluorescence immunohistochemistry procedures were performed as described earlier (Madhavarao et al., 2004), with minor modifications.

Dual-labeling fluorescence immunohistochemistry was done with the affinity-purified antipeptide AceCS1 anti-

bodies diluted 1:500 or with antirecombinant protein antibodies diluted 1:1,000. These were used together with either an oligodendrocyte marker antibody directed against the tumor suppressor protein adenomatous polyposis coli (CC1) or an astrocyte marker antibody against glial fibrillary acidic protein (GFAP). The CC1 oligodendrocyte marker was a mouse monoclonal antibody (Chemicon International, Temecula, CA; No. OP80) that was used at a dilution of 1:100. This antibody has been used previously to localize oligodendrocytes (Papay et al., 2006) and was found to stain cells with oligodendrocyte morphology throughout the white matter and in some gray matter areas such as the deeper layers of neocortex. The astrocyte maker was a rat monoclonal antibody (Zymed, Invitrogen, Carlsbad, CA; No. 13-0300) and was used at a dilution of 1:100. This GFAP antibody stained cells with typical astrocyte morphology in both gray and white matter, and staining was completely excluded from the cell nuclei. Primary antibodies were diluted in PBS with 0.3% Triton X-100. See Table 1 for primary antibody details. The secondary antibodies used for these primary marker antibodies were goat anti-rabbit coupled with Alexa Fluor 488 (1:100; Invitrogen) and goat anti-mouse coupled with Alexa Fluor 594 (1:100; Invitrogen). Appropriate controls included elimination of primary antibodies as well as the use of each primary antibody separately. The fluorochromes for the secondary antibodies were chosen such that AceCS1 immunoreactivity would fluoresce green and all the other marker immunoreactivities would give a red fluorescence. DAPI nuclear stain (Vector, Burlingame, CA) was used to visualize cell nuclei with blue fluorescence. Slides incubated without primary antibody showed no fluorescence when treated with secondary antibodies alone.

The immunofluorescence was visualized under  $\times 20$ ,  $\times 40$ , and  $\times 100$  objectives on a laser scanning confocal microscope (LSCM; Zeiss Pascal) using three lasers with peak wavelengths allowing excitation of red, green, and blue fluorochromes. The scanned images were

superimposed and analyzed in image analysis software (LSCM Image Browser version 5). Double-labeled cells appeared yellow to orange (for red and green fluorochromes), or magenta (for blue and red fluorochromes), and triple-labeled cells appeared white (red, blue, and green fluorochromes).

### Controlled cortical impact injury

Male Sprague-Dawley rats (200–250 g) were obtained from Charles River Laboratories (Raleigh, NC). All procedures were performed in accordance with guidelines of the National Institutes of Health and the Institutional Animal Care and Use Committee. Animals were housed on a 12-hour reversed light–dark cycle.

Rats were anesthetized with 4% isoflurane vaporized in O<sub>2</sub> and maintained with 2% isoflurane during surgery. The head was fixed in a stereotaxic frame (David Kopf instruments, Tujunga, CA), and after retracting the scalp an 8-mm craniotomy was made over the left parietal cortex, 0.5 mm posterior to the coronal suture and 3 mm lateral to the sagittal suture. Care was taken to avoid injury to the dura, which was continuously bathed in sterile physiological saline during the procedure. Controlled cortical impact (CCI) injury was produced by a single impact with a CCI device (Pittsburgh Precision Instruments, Pittsburgh PA) with a 6-mm flat steel impact tip (5 m/second, 2.5 mm deformation). Impact velocity was measured for reproducibility. Immediately after the injury, the bone flap was replaced and sealed with dental acrylic cement, and the scalp and skin were closed with staples.

### Peroxidase immunohistochemistry

Four female adult rats, three 18-day-old female rats, and two CCI-injured adult male rats (Sprague Dawley) were deeply anesthetized and perfused transcardially with 4% paraformaldehyde. Brains were postfixed for several hours in 4% paraformaldehyde before being passed through a series of 10%, 20%, and 30% sucrose solutions. Coronal brain slices 4 mm thick were embedded in OCT compound on microtome chucks and frozen rapidly with compressed difluoroethane gas. Sections were cut at a thickness of 20 µm in the coronal plane at a temperature of –18°C. Free-floating tissue sections were collected and washed in PBS and then incubated for 30 minutes with 1:1 methanol/water containing 1% H<sub>2</sub>O<sub>2</sub> to block endogenous peroxidase. Tissue sections were blocked against nonspecific antibody binding by incubating with PBS containing 2% NGS and 0.1% sodium azide and were stored in the same solution at 4°C until use. The sections were then processed for immunoperoxidase histochemistry by the avidin-biotin complex (ABC) method, with horseradish peroxidase as the enzyme marker (Vectastain Elite; Vector).

Sections were incubated with either affinity-purified anti-AceCS1 peptide antibodies (1:1,000–1:1,300 range) or crude antibodies against the full-length protein (1:5,000–1:10,000 range) in PBS containing 2% NGS plus 0.1% sodium azide. Sections were incubated in 35-mm culture dishes overnight with slow, constant rotary agitation on an orbital shaker. Tissue sections were washed in PBS and treated with biotinylated secondary antibody in 2% NGS/PBS for 90 minutes. Sections were washed again in PBS and treated with the avidin-peroxidase complex solution containing 0.5% bovine serum albumin for 90 minutes. After thorough washing in PBS, tissue sections were developed using a nickel and cobalt enhanced diaminobenzidine chromogen (Pierce). After the final wash in distilled water with 0.01% bovine serum albumin, the tissue sections were transferred to treated slides (Superfrost Plus; Thermo Fisher Scientific, Waltham MA), dried at 50°C, dehydrated in an ethanol series, cleared in xylene, and mounted with cover glasses and cyto seal-60 (Richard Allen Scientific Inc., Kalamazoo, MI). Images were acquired with a DIC-equipped Olympus BX51 microscope and Olympus DP71 camera and were adjusted for brightness and contrast in PC-based imaging software (Media Cybernetics, Silver Spring, MD, and Adobe Systems, San Jose, CA).

Antibody blocking studies were performed by incubating the affinity-purified peptide antibodies, diluted to 1:1,300, with 10 µg/ml of the immunization peptide overnight at 4°C before applying to the tissue sections. Antibodies against the full-length protein were similarly blocked by incubating the antibodies, diluted 1:5,000, with 10 µg/ml of the recombinant AceCS1 protein for 6 hours at 4°C prior to applying to fixed tissue sections. Tissue sections were then processed by the ABC method and developed as described above.

## RESULTS

### Western blotting

The rabbit polyclonal antibodies raised against a synthetic mouse N terminal 18-mer peptide sequence from AceCS1 were found to react predominantly with a close doublet of protein bands corresponding to approximately 76 kD in the Western blots of rat brain homogenates. Figure 1 shows a strongly reactive pair of protein bands with crude anti-AceCS1 sera, indicating that the unpurified antibody preparation was relatively specific. An additional immunoreactive band was seen at a molecular weight of approximately 38 kD, along with other minor bands. After affinity purification, the antibody specificity toward AceCS1 was increased, with substantial reduction of the 38-kD immunoreactive band and near elimination of the minor reactive bands.

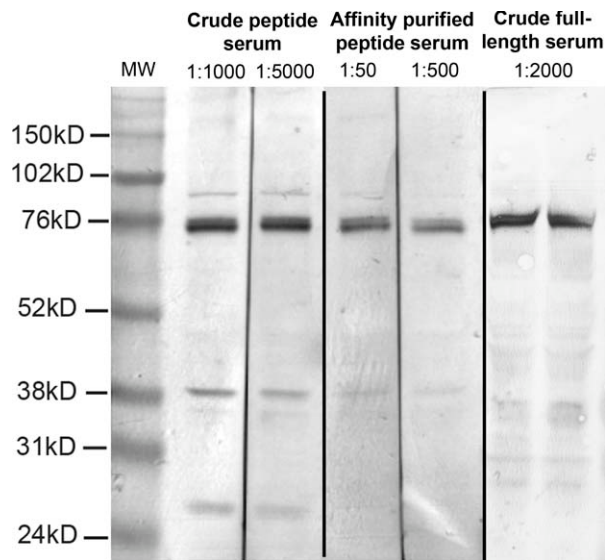


**Figure 1.** Western blots depicting anti-peptide AceCS1 antibody specificity before and after affinity purification and the immunoreactivity with the crude antisera directed against full-length recombinant AceCS1 protein. Both antibodies reacted with a doublet band at approximately 76 kD. The anti-peptide antibody also reacted with several minor bands, which were mostly removed by affinity purification.

The polyclonal antibodies raised against the full-length recombinant protein also reacted with a close doublet of bands at an estimated molecular weight of approximately 76 kD and showed slight immunoreactivity with other bands. Both antibodies were found to be suitable for immunohistochemistry, but the antibody directed against the full-length recombinant protein provided greater signal to background staining in paraformaldehyde-fixed brain sections. Furthermore, the two antibodies displayed somewhat different staining patterns. The anti-recombinant AceCS1 protein antibodies stained cell nuclei more strongly and stained a greater number of nuclei than the anti-peptide AceCS1 antibodies. The anti-peptide antibodies stained fewer nuclei and generally stained them more lightly than the antisera against the full-length protein, but they also showed immunoreactivity with more neuronal cell bodies scattered throughout the brain. In addition, the anti-peptide antibodies stained small, punctate structures on the surface of neuronal cell bodies in select areas of the brain, including hippocampus, neocortex, and piriform cortex. The antibody against the recombinant protein did not show as much cytoplasmic staining in subpopulations of neurons or the punctate structures on the surface of neurons. The reason for the discrepancy, in which the anti-protein antibody preferentially stained cell nuclei and the anti-peptide antibody preferentially stained cytoplasm, may be differential posttransla-

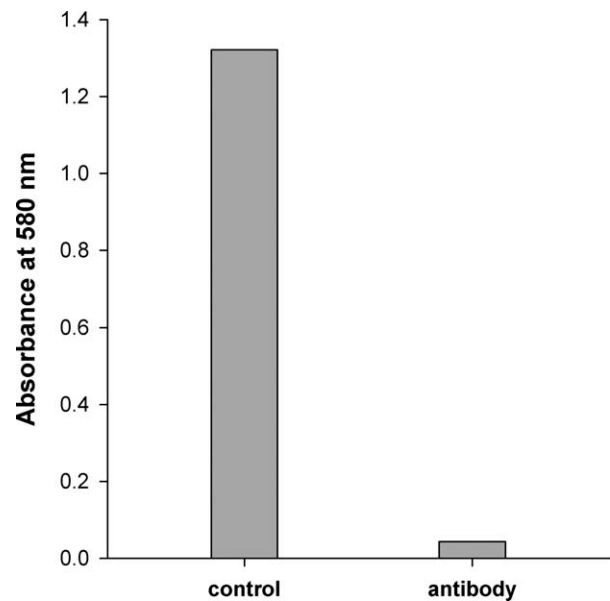


**Figure 2.** AceCS1 immunoprecipitation studies showed that the affinity-purified anti-peptide antibody removed most of the AceCS1 enzymatic activity from brain homogenates. Less than 4% of the activity in the control samples was present in the samples immunoprecipitated with the anti-peptide AceCS1 antibody.

tional modification of the N-terminus of AceCS1 in the two cellular compartments.

### Immunoprecipitation

Immunoprecipitation assays were done with the affinity-purified AceCS1 antibodies in order to determine the extent to which they could remove AceCS1 enzymatic activity from solution. Brain homogenates were incubated with the antibodies before being precipitated with protein-G agarose beads, and the resultant supernatants were assayed for AceCS1 activity. Figure 2 shows the absorbance of the pyrophosphate-molybdate product at 580 nm in control and experimental samples. The mean values of three successive readings of the same sample are given (assays done in duplicates). The results show that less than 4% of the activity remained in the supernatant of the immunoprecipitated fractions compared with the BSA controls, confirming that the antibody reacts with AceCS1 protein.

### Immunofluorescence colocalization in rat brain

To colocalize AceCS1 enzyme expression with other markers, we employed double-labeling immunofluorescence histochemistry with oligodendrocyte and astrocyte markers (CC1 and GFAP respectively; see Materials and Methods and Table 1). Cell nuclei were stained for AceCS1 throughout the brain and spinal cord. Subsets of

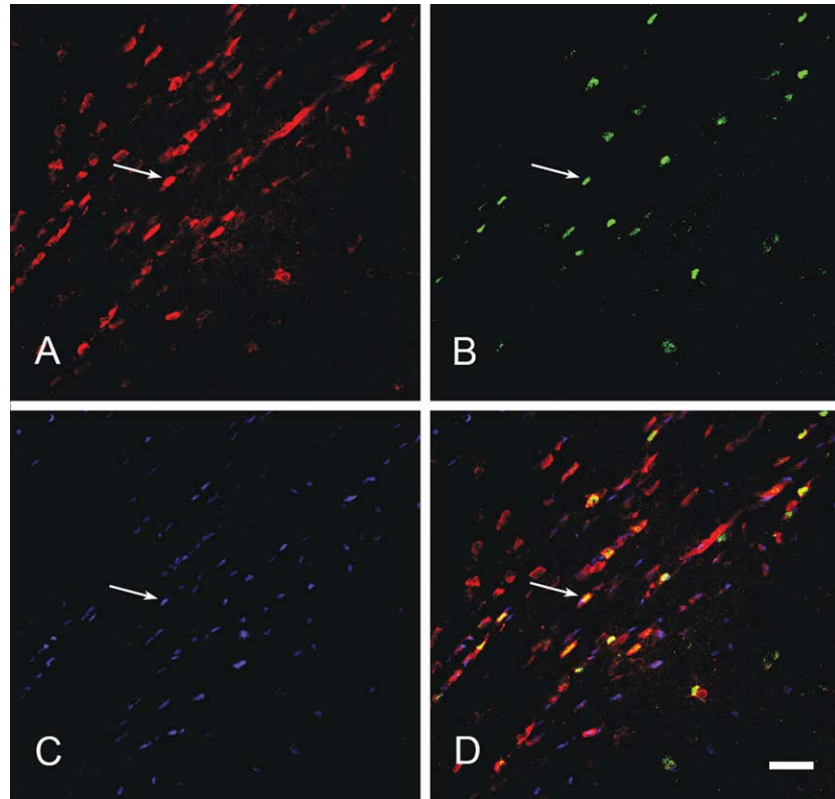


**Figure 3.** AceCS1 antipeptide antibody colocalization with the oligodendrocyte marker CC1 in the corpus callosum using the antipeptide AceCS1 antibodies. **A:** CC1 immunoreactivity (red). **B:** AceCS1 immunoreactivity (green). **C:** DAPI fluorescence showing cell nuclei (blue). **D:** Merged image. A magenta color shows colocalization of AceCS1 with cell nuclei, whereas a yellow to white color shows colocalization of AceCS1 with both cell nuclei and CC1 (arrows show the same cell in all four panels). Scale bar = 25  $\mu$ m.

both neurons and oligodendrocytes were immunoreactive for AceCS1, with the majority of both cell types being nonreactive in adult rats. Figure 3 shows the colocalization of AceCS1 with the oligodendrocyte marker CC1 in the corpus callosum in the adult rat brain. Figure 3A is an image of CC1 immunoreactivity in the corpus callosum showing oligodendrocytes, and Figure 3B shows AceCS1 immunoreactivity (AceCS1-IR) in the same field. Figure 3C is the DAPI fluorescence signal for cellular nuclei, and Figure 3D is the merged image showing all three markers. In this image, AceCS1 immunoreactivity was apparent in both the cytoplasm and the nuclei of a subset of the CC1-labeled oligodendrocytes, but the nuclear expression was typically much stronger than that in the cytoplasm. The fimbria of the hippocampus contained a higher proportion of AceCS1-immunoreactive oligodendrocytes than the corpus callosum (Fig. 4A–D). In the fimbria, most CC1-labeled oligodendrocytes were also AceCS1 positive (Fig. 4D). Figure 5 shows AceCS1 and CC1 immunoreactivities in neocortex, demonstrating that many of the stained cell nuclei in the deeper layers of neocortex belonged to oligodendrocytes.

Fluorescence colocalization with the recombinant AceCS1 antibody and GFAP, a marker for astrocytes, could not unequivocally demonstrate coexpression of the two markers in astrocytes (Fig. 6A–H). AceCS1 stained cell nuclei intensely, whereas the GFAP antibodies stained astrocyte processes, and, although the two immunoreactivities were closely associated, they were nonoverlapping to a great extent. GFAP-positive astrocyte processes were very closely associated with AceCS1-immunoreactive cell nuclei, but, because the GFAP antibodies stained only astrocyte processes and the recombinant AceCS1 protein antibodies stained cell nuclei most intensely, it was difficult to determine whether the two markers were expressed in the same cells or adjacent cells. With z-series images at different depths through tissue slices, it was evident that astrocyte processes often surrounded AceCS1-immunoreactive cell nuclei in areas rich in astrocytes, such as the glia limitans at the brain surface (see Fig. 6E,H; see also Supp. Info. Fig. 1). The glia limitans contains astrocytes almost exclusively and also exhibited some of the highest density of stained glial cell nuclei. We conclude that many of the AceCS1-

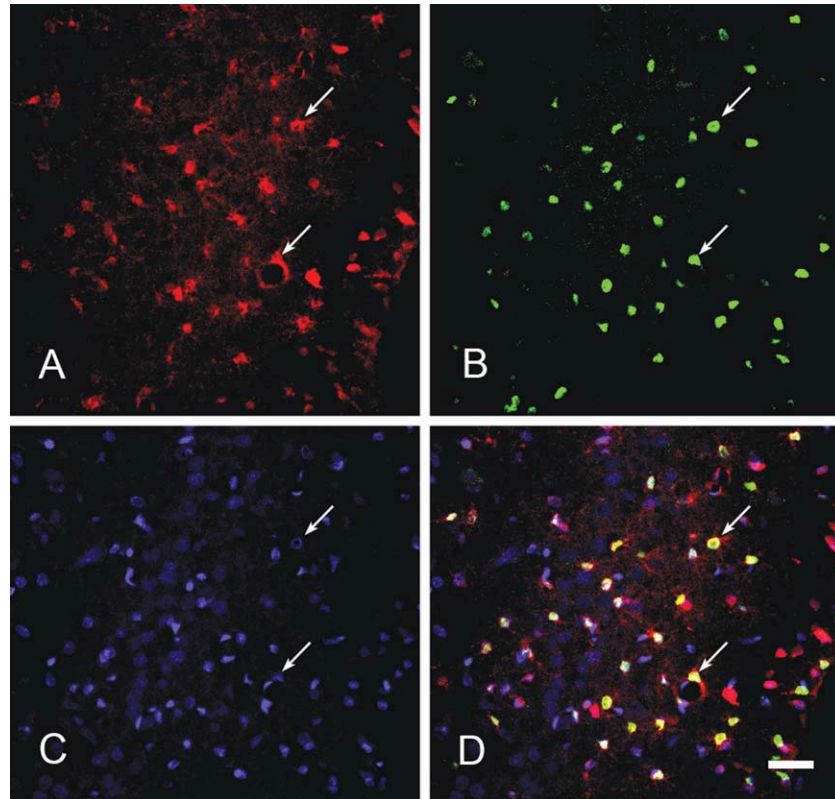


**Figure 4.** AceCS1 antipeptide antibody colocalization with oligodendrocyte marker CC1 in the fimbria of the hippocampus. Affinity-purified antipeptide antibodies were used. **A:** CC1 immunoreactivity with red fluorochrome. **B:** AceCS1 immunoreactivity with green fluorochrome. **C:** DAPI fluorescence showing cell nuclei in blue. **D:** Merged image. A magenta color shows colocalization of AceCS1 with cell nuclei, whereas a yellow to white color shows colocalization of AceCS1 with both cell nuclei and CC1. Arrows indicate the same cells in the four panels. Scale bar = 25  $\mu\text{m}$ .

immunoreactive cell nuclei at the brain surface belonged to the astrocytes that make up the glia limitans and that some of the other immunoreactive cell nuclei in other areas of the brain also belonged to astrocytes.

### Peroxidase-based immunohistochemistry for AceCS1

Peroxidase avidin-biotin complex immunohistochemistry in the adult rat brain showed AceCS1-IR to be localized predominantly in cell nuclei scattered throughout the brain and spinal cord. However, these stained cell nuclei were not homogeneously distributed but instead were more concentrated in certain brain areas and at the brain surface. Other brain regions had notably lower density of immunoreactive cell nuclei. Two different patterns of immunoreactivity were observed in cell nuclei. The nuclei of some nonneuronal cells were small, typically round or oval, and intensely stained. This contrasted with AceCS1 expression in neuronal nuclei, which when stained were lightly to moderately immunoreactive, often with an uneven distribution throughout the nucleus. Subpopula-

tions of oligodendrocytes and neurons also expressed AceCS1 at low levels in their cytoplasm. Furthermore, a significant number of neurons and axons were immunoreactive in the brainstem. The pattern of immunoreactivity by region is given below.

### Antibody blocking studies

The specificities of the affinity-purified peptide anti-AceCS1 and full-length recombinant protein antibodies were demonstrated by antigen blocking studies. The immunoreactivity in brain tissue slices was eliminated by preadsorption of working dilutions of the affinity-purified anti-AceCS1 peptide antibody with 10  $\mu\text{g}/\text{ml}$  synthesized AceCS1 N-terminal peptide of murine AceCS1 (Fig. 7A,B). Similarly, the immunoreactivity of the antibodies against full-length AceCS1 was blocked by preincubation with 10  $\mu\text{g}/\text{ml}$  of the recombinant protein (Fig. 7C,D).

### Forebrain fiber tracts

AceCS1-IR was variable among oligodendrocytes in the white matter of adult rats, with a subpopulation

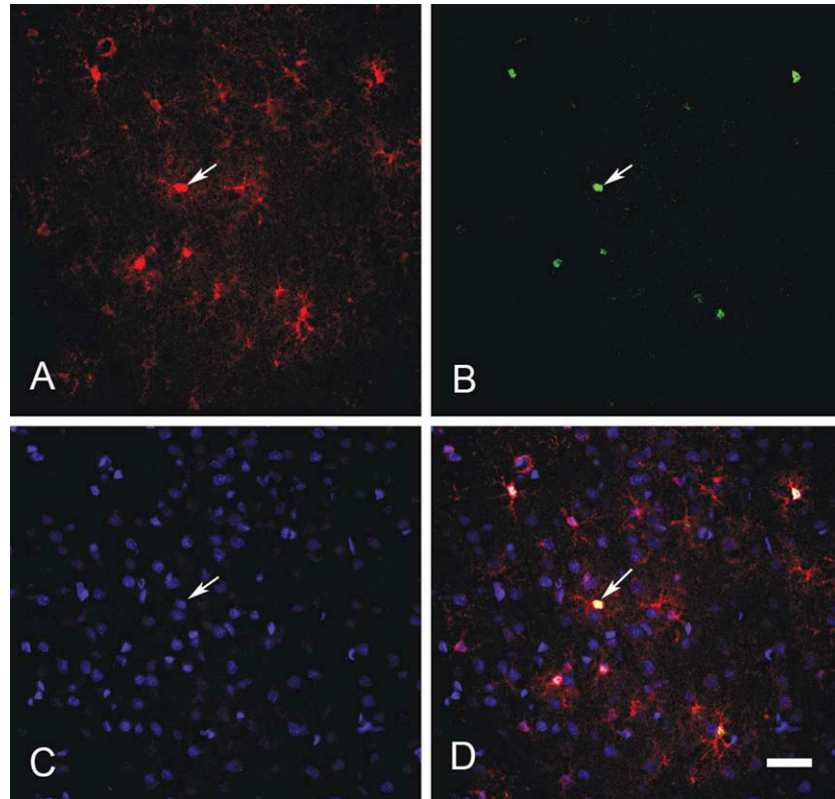


**Figure 5.** Antipeptide AceCS1 antibody colocalization with oligodendrocyte marker CC1 in layer IV of temporal cortex. The expression in this area colocalized with both CC1 and DAPI, indicating that AceCS1 was present in the nuclei of oligodendrocytes. Arrows show fluorescence with all three markers, and the colocalization in the merged image. **A:** CC1 immunoreactivity. **B:** AceCS1 immunoreactivity. **C:** DAPI fluorescence showing cell nuclei. **D:** Merged image. Arrows indicate the same cell in each image. Scale bar =  $\sim 25 \mu\text{m}$ .

expressing strong immunoreactivity in their nuclei and only faint staining or no staining in their cytoplasm (Fig. 8). In forebrain, AceCS1-immunoreactive oligodendrocytes were observed in all fiber pathways, including the corpus callosum (Fig. 8A,F; cc), internal capsule (Fig. 8B; int), optic tract (Fig. 8C; opt), anterior commissure (Fig. 8D; ac), lateral olfactory tract (Fig. 8E; lot), and fimbria and hippocampal commissure (Fig. 8F; fim, vhc). Immunoreactive oligodendrocytes invariably stained more strongly in their nuclei than in their cytoplasm.

### Neocortex

In the adult rat brain, AceCS1 was expressed most strongly in scattered cell nuclei in all layers of neocortex (Fig. 9A). Immunoreactive cell nuclei were also observed in white matter, such as the corpus callosum (Fig. 9B). The immunoreactive intensity in cell nuclei varied widely, some of the nuclei being intensely stained and others being only very lightly stained (Fig. 9C). The intensely stained cell nuclei were observed in all cortical layers and were often present in closely associated pairs (Fig. 9D).

Many of the very lightly stained nuclei were those of neurons, including cortical pyramidal cells (Fig. 9C). A small number of ependymal cells and endothelial cells also had immunoreactive nuclei.

Light to moderate cytoplasmic staining was present in some neurons, oligodendroglia, and ependymal cells, but the majority of these cell types did not express AceCS1 in their cytoplasm. Astrocytes did not express detectable levels of AceCS1 in their cytoplasm. However, the subpial surface of the brain, which comprises the glia limitans, exhibited a high density of strongly immunoreactive cell nuclei (Fig. 9E; see also Figs. 12C,D, 13BC). Astrocytes are the predominant cell type present in the glia limitans, suggesting that the strongly immunoreactive cell nuclei at the brain surface belonged to astrocytes. The anti-AceCS1 peptide antibody differed slightly in the staining pattern from the antibodies raised against the full-length recombinant protein. One feature of the staining pattern that was unique to the antipeptide antibodies was that they stained small ( $\sim 0.5\text{--}1 \mu\text{m}$ ), punctate structures on the surface of neuronal cell bodies and dendrites in cortex, hippocampus, and other brain regions. These

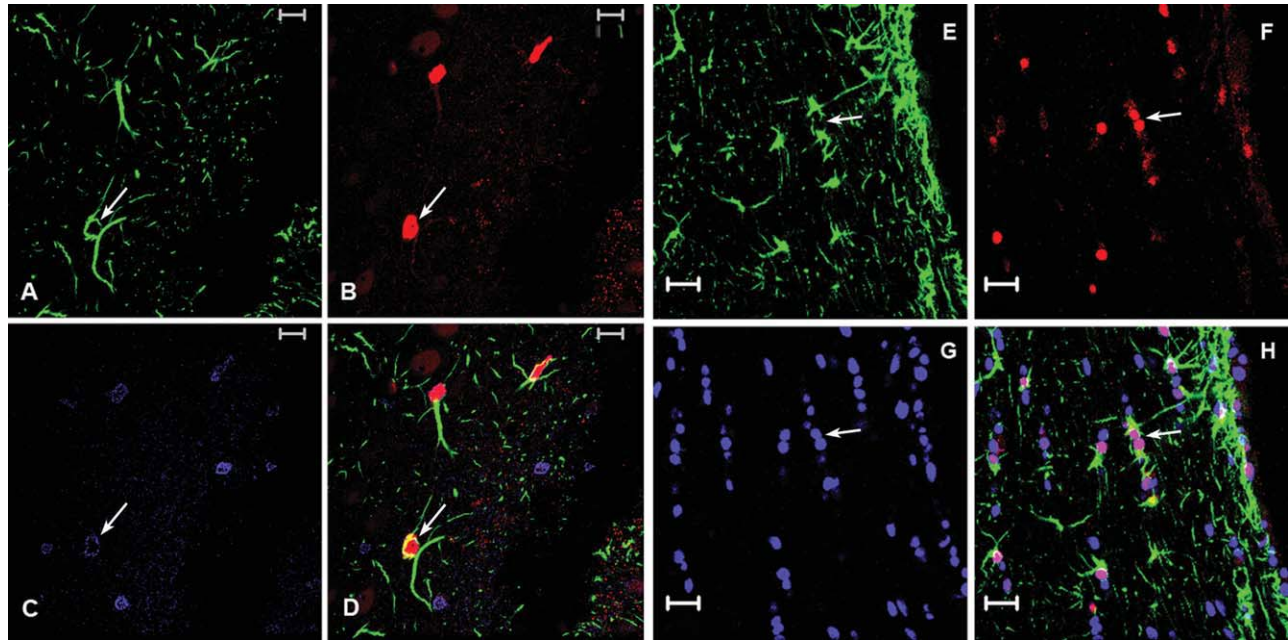


**Figure 6.** AceCS1 antirecombinant protein antibody colocalization with the astrocyte marker GFAP in layer VI of neocortex (A–D) and at the brain surface, including glia limitans (E–H). AceCS1 expression (red) was colocalized with DAPI (blue), resulting in a magenta color (arrows in D,H), indicating that AceCS1 was present in the nuclei of cells. It was difficult to determine whether GFAP (green) and AceCS1 were colocalized in the same cells as a result of nonoverlapping distributions in astrocyte processes and cell nuclei, respectively. However, the pattern of immunoreactivities for the two markers was consistent with localization AceCS1 in the nuclei of some astrocytes. Scale bars = 10  $\mu\text{m}$  in A–D; 20  $\mu\text{m}$  in E–H.

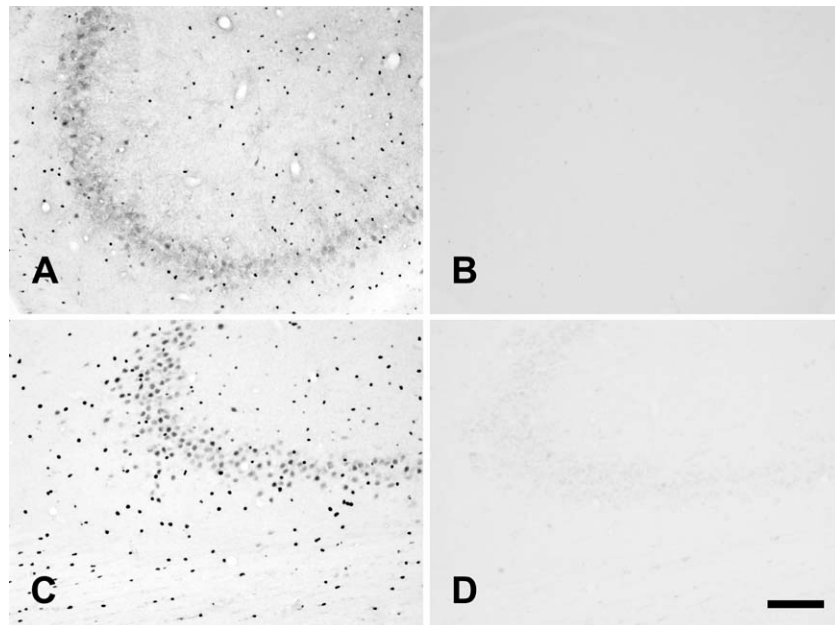


**Figure 7.** AceCS1 antibody blocking studies. AceCS1 immunoreactivity was blocked by preincubation of the antipeptide antibodies (1:1,300 dilution) with 10  $\mu\text{g}/\text{ml}$  of the immunizing peptide. For example, AceCS1-IR in the CA3 region of hippocampus (A) was completely blocked by preincubating the antipeptide antibodies with the immunizing peptide (B). AceCS1-IR with the antirecombinant protein antisera (diluted 1:5,000) was blocked in the CA3 region of hippocampus from the same rat by preincubating the antirecombinant antisera with 10  $\mu\text{g}/\text{ml}$  of the recombinant protein used for immunizations (C,D). Scale bar = 120  $\mu\text{m}$ .

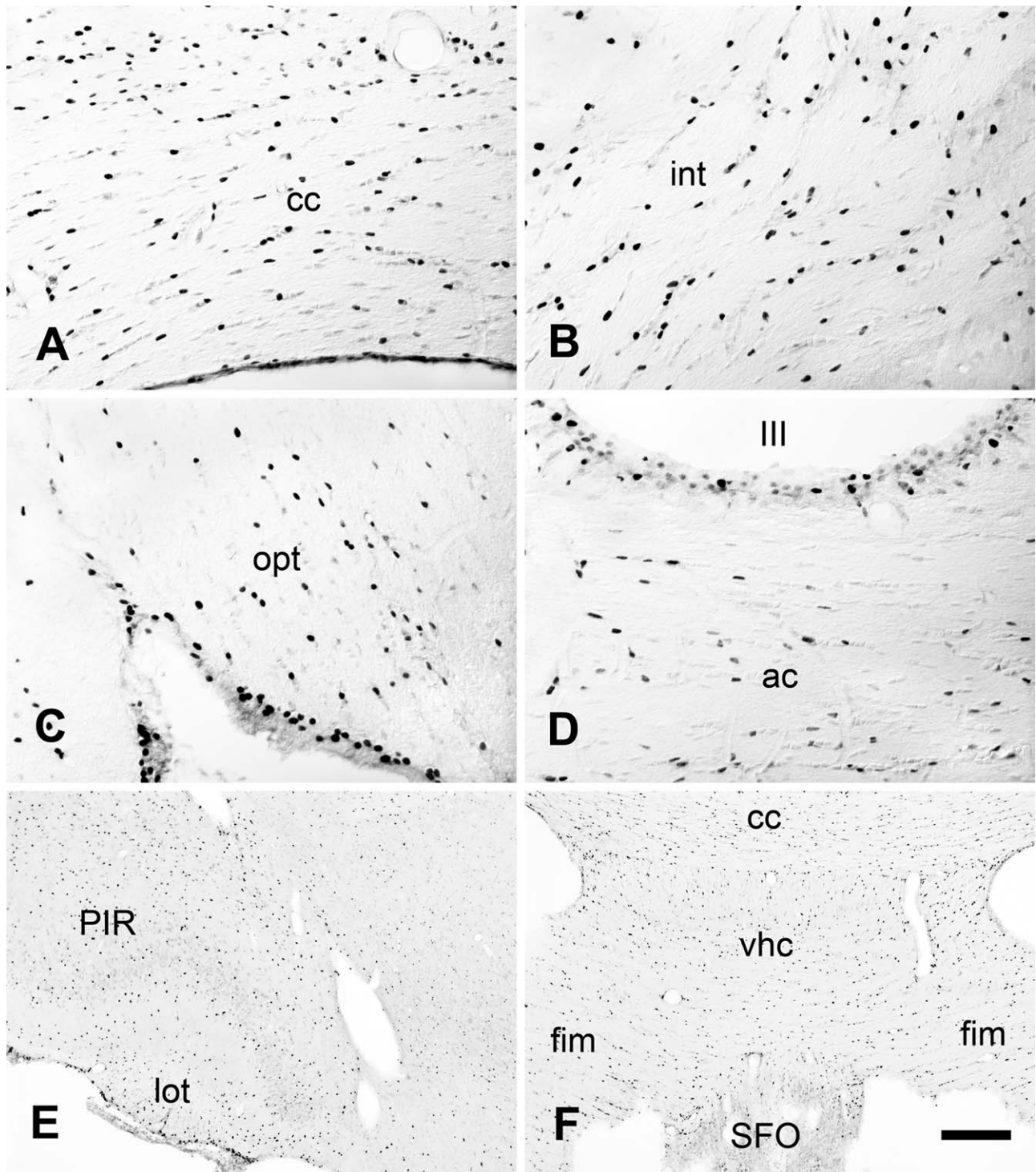


**Figure 8.** AceCS1-IR in forebrain fiber tracts. Some oligodendrocyte nuclei were strongly immunoreactive for AceCS1 in all fiber tracts, including in the corpus callosum (cc; A,F), internal capsule (int; B), optic tracts (opt; C), anterior commissure (ac; D), lateral olfactory tract (lot; E), fimbria (fim; F), and ventral hippocampal commissure (vhc; F). Light cytoplasmic staining was observed in some oligodendrocytes, but most were unstained. Ependymal cell nuclei, for example, those around the third ventricle (III), were also variably stained for AceCS1 (D). SFO, subfornical organ. A–D were acquired with DIC optics (images adjusted for evenness of illumination). All images from tissue stained with antirecombinant protein AceCS1 antibodies. Scale bar = 300  $\mu$ m in F (applies to E,F); 60  $\mu$ m for A–D.

immunoreactive puncta were not seen with the recombinant protein antibodies. For example, the recombinant protein antibodies stained only cellular nuclei in layers I–

III of neocortex (Fig. 9E), whereas the antipeptide antibodies stained cellular nuclei, scattered interneurons, and small puncta on the surface of neurons (Fig. 9F).

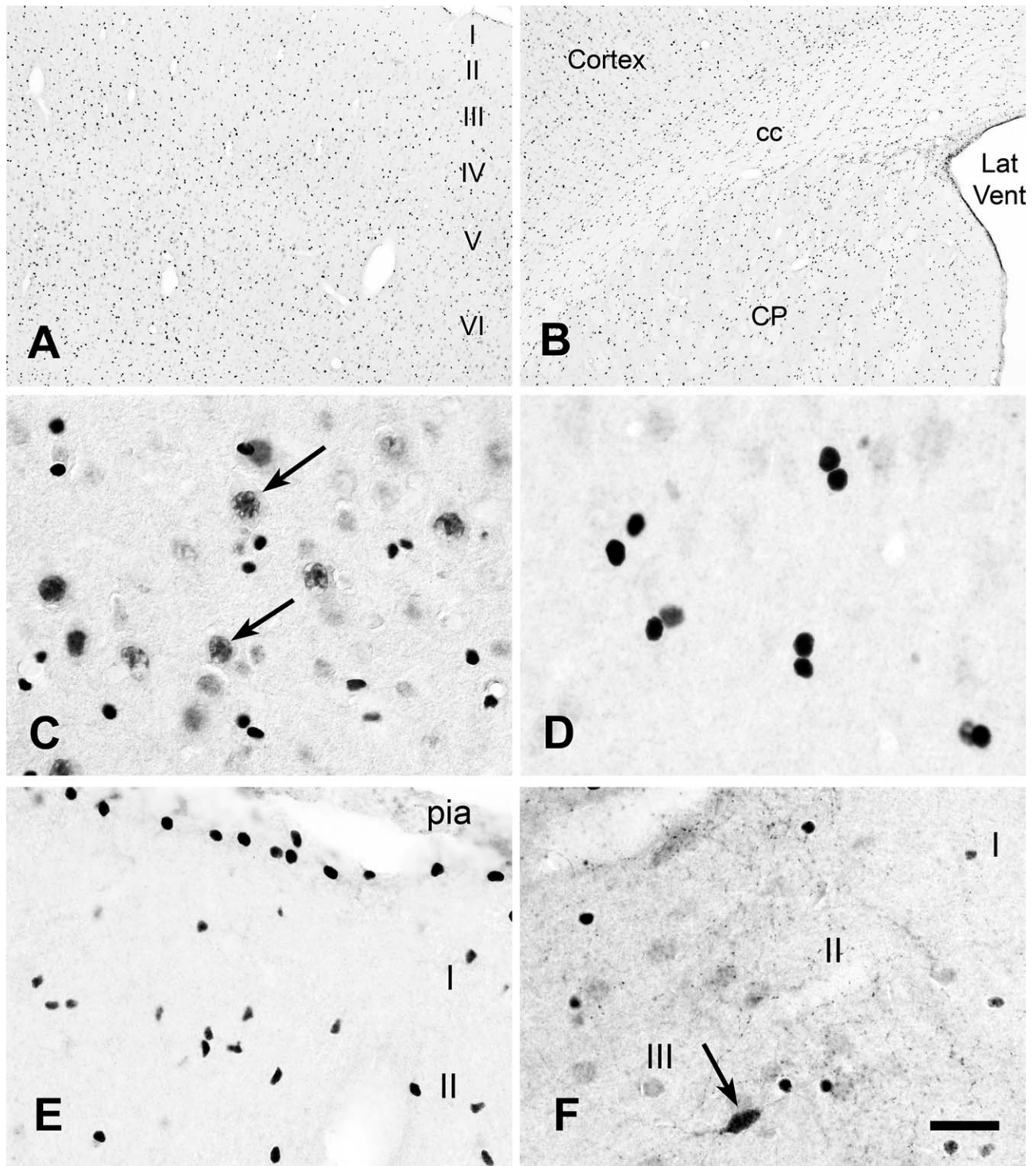


**Figure 9.** Neocortex. AceCS1 was expressed in all layers of neocortex (A) as well as in underlying structures including the corpus callosum (cc) and striatum (caudate/putamen; CP; B). The most strongly immunoreactive elements were cellular nuclei. In general, neuronal nuclei, such as motor neurons in layer V of cortex, tended to express lower levels of AceCS1 (arrows) than was observed in small nonneuronal cells, and the staining was unevenly distributed within the nuclei (C). The small, strongly immunoreactive cell nuclei were often observed in closely associated pairs, such as in layer IV of neocortex (D). Cell nuclei in layer I of neocortex were numerous and strongly stained at the surface but were less numerous and less strongly immunoreactive in the remainder of layer I (E). Unlike the antiprotein AceCS1 antibody, the antibody generated against the peptide sequence stained more neurons (arrow) and stained puncta in areas such as layers II and III of neocortex (F). A-E: protein antibody; F: affinity-purified peptide antibody. Scale bar = 30  $\mu$ m in F (applies to C,E,F); 300  $\mu$ m for A,B; 20  $\mu$ m for D.

### **Hippocampus**

The predominant immunoreactive elements observed with the recombinant protein antibodies in the adult rat hippocampus were strongly immunoreactive cellular nuclei present in all layers (Fig. 10A,B). These immunoreactive cell nuclei were most densely concentrated at the border between the granule cell and the polymorph layers in the dentate gyrus (Fig. 10F). Additionally, the nuclei of CA3 pyramidal neurons were lightly to moderately immunoreactive (sp layer in Fig. 10F; see also Fig. 7C), whereas the nuclei of pyramidal neurons in other regions were either unstained or faintly stained.

The antipeptide AceCS1 antibodies also stained cell nuclei in all layers of hippocampus (Fig. 10C,D), but in addition stained a small number of scattered interneurons as well as numerous small puncta on the surface of neurons (Fig. 10E). The immunoreactive puncta were particularly concentrated on the cell bodies and processes of hippocampal pyramidal neurons.

### **Telencephalic nuclei**

The telencephalic nuclei, including the caudate-putamen (CP), globus pallidus (GP), and amygdala, contained numerous moderately to strongly immunoreactive cell nuclei (Fig. 11). The staining patterns with the two antibodies were similar in the CP (Fig. 11A,B). A greater density of immunoreactive cell nuclei was observed in the CP than in the GP (Fig. 11C), and, similarly to neocortex, immunoreactive cell nuclei in the CP were often present in closely associated pairs (Fig. 11D). AceCS1 immunoreactivity was relatively low in the substantia innominata (Fig. 11E). Numerous immunoreactive cell nuclei were present throughout the amygdala (Fig. 11F).

### **Septum, diagonal band, and piriform cortex**

AceCS1-IR using the recombinant protein antibodies was present primarily in cell nuclei in the medial and lateral septum (Fig. 12A). In addition to staining cellular nuclei, the antipeptide antibodies also stained neurons and numerous puncta in the septum (Fig. 12B). In the horizontal diagonal band of Broca, the recombinant protein antibodies stained some nonneuronal cellular nuclei strongly and stained neurons only very slightly (Fig. 12C). In contrast, the antipeptide AceCS1 antibodies also stained diagonal band neurons lightly to moderately (Fig. 12D). In piriform cortex, the antipeptide antibodies stained some nonneuronal cellular nuclei strongly and neuronal nuclei very faintly (Fig. 12E). The antipeptide antibodies also stained scattered interneurons and many small puncta in piriform cortex, especially in the pyramidal cell layer (Fig. 12F).

### **Midbrain**

AceCS1-IR was present in many cellular nuclei in the periaqueductal gray (Fig. 13A) as well as the ventral tegmental area and medial mammillary nucleus (Fig. 13B,C). The density of immunoreactive cell nuclei was greater in the substantia nigra compact cell division than in the reticular portion (Fig. 13C,D). Primary sensory neurons of the mesencephalic nucleus of the trigeminal nerve expressed the highest level of cytoplasmic AceCS1 in the brain (Fig. 13E,F). The strongest immunoreactivity in these sensory neurons was present in the vicinity of the nuclear membrane (Fig. 13F).

### **Cerebellum and pons**

Relatively low AceCS1-IR was present in cerebellar cortex, which is consistent with a previous report showing low AceCS activity in the cerebellum (Szutowicz and Lysiak, 1980). AceCS1-IR in the cerebellum was expressed in some Purkinje cell and Bergman cell nuclei and scattered cell nuclei in the molecular and granule cell layers (Fig. 14A,B). Purkinje cells ranged from unstained to lightly immunoreactive, with prominent localization in the cell nucleus (Fig. 14C,D). Granule cells were mostly unstained, but a small percentage of cell nuclei in the granule cell layer was moderately to strongly immunoreactive (Fig. 14B,C). The pontine gray was notable for having an exceptionally high density of strongly stained cell nuclei, which were interspersed among much more lightly stained neurons (Fig. 14E,F).

### **Brainstem**

The primary sensory neurons of the vestibular ganglia expressed moderate to strong cytoplasmic AceCS1-IR (Fig. 15A,B), as was the case with the sensory neurons of the mesencephalic nucleus of the trigeminal nerve (see Fig. 13F). The expression of AceCS1 in these sensory neurons was variable between cytoplasmic and nuclear compartments, with some cells having greater expression in the cytoplasm and others having greater expression in the nucleus (Fig. 15B). Many axons and oligodendrocytes making up the nerves and fiber tracts exhibited light to moderate immunoreactivity (Fig. 15C). Oligodendrocytes tended to stain strongly in the cell nucleus and lightly to moderately in the cytoplasm. Some large brainstem neurons, including those in the lateral vestibular, trigeminal, cochlear, and reticular nuclei, had light to moderate cytoplasmic AceCS1 expression, and the expression was often strongest in the perinuclear region of the immunoreactive neurons (Fig. 15D). Many axons in the brainstem were lightly to moderately immunoreactive for AceCS1, including those of the tectospinal tract, medial longitudinal fasciculus, and eighth cranial nerve (Fig. 15C,E,F).

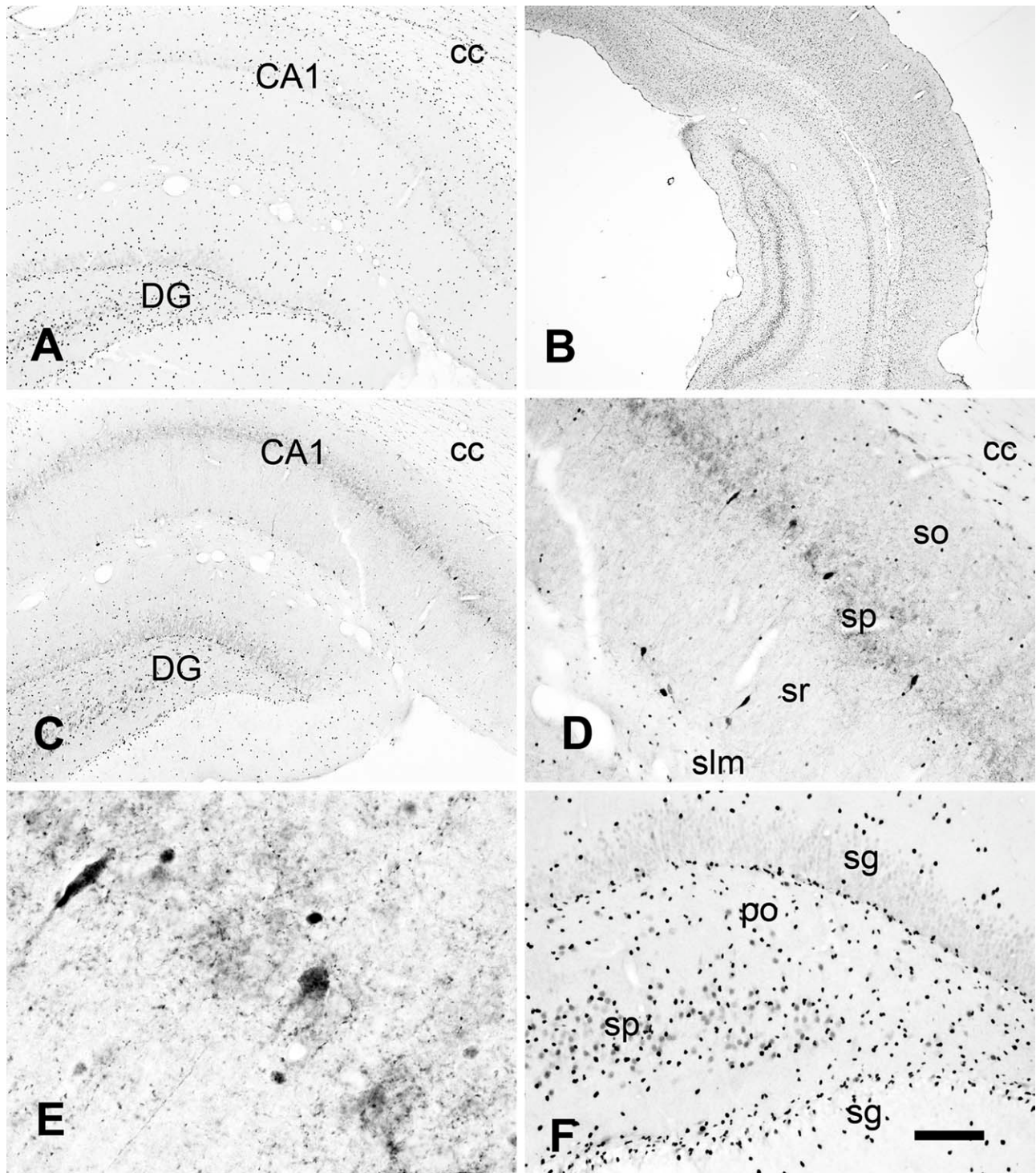


**Figure 10.** Hippocampus. The antirecombinant AceCS1 protein antibodies stained cellular nuclei in all layers of hippocampus. The dorsal hippocampus is shown in A, and the caudal hippocampus is shown at low magnification in B. The immunoreactive cell nuclei were most concentrated in CA3 and the border between the granule cell (sg) and polymorph (po) layers (F). The antipeptide AceCS1 antibodies stained fewer nuclei but also stained scattered interneurons and numerous puncta, which was not seen with the protein antibody (compare images A and C; D,E are successive enlargements of the area shown in C). cc, Corpus callosum; DG, dentate gyrus; sg, granule cell layer; po, polymorph layer; slm, stratum lacunosum moleculare; so, stratum oriens; sp, stratum pyramidal CA3; sr, stratum radiatum. A,B,F: protein antibody; C–E: affinity-purified peptide antibody. Scale bar = 120  $\mu$ m in F (applies to D,F); 300  $\mu$ m for A,C; 1 mm for B; 30  $\mu$ m for E.

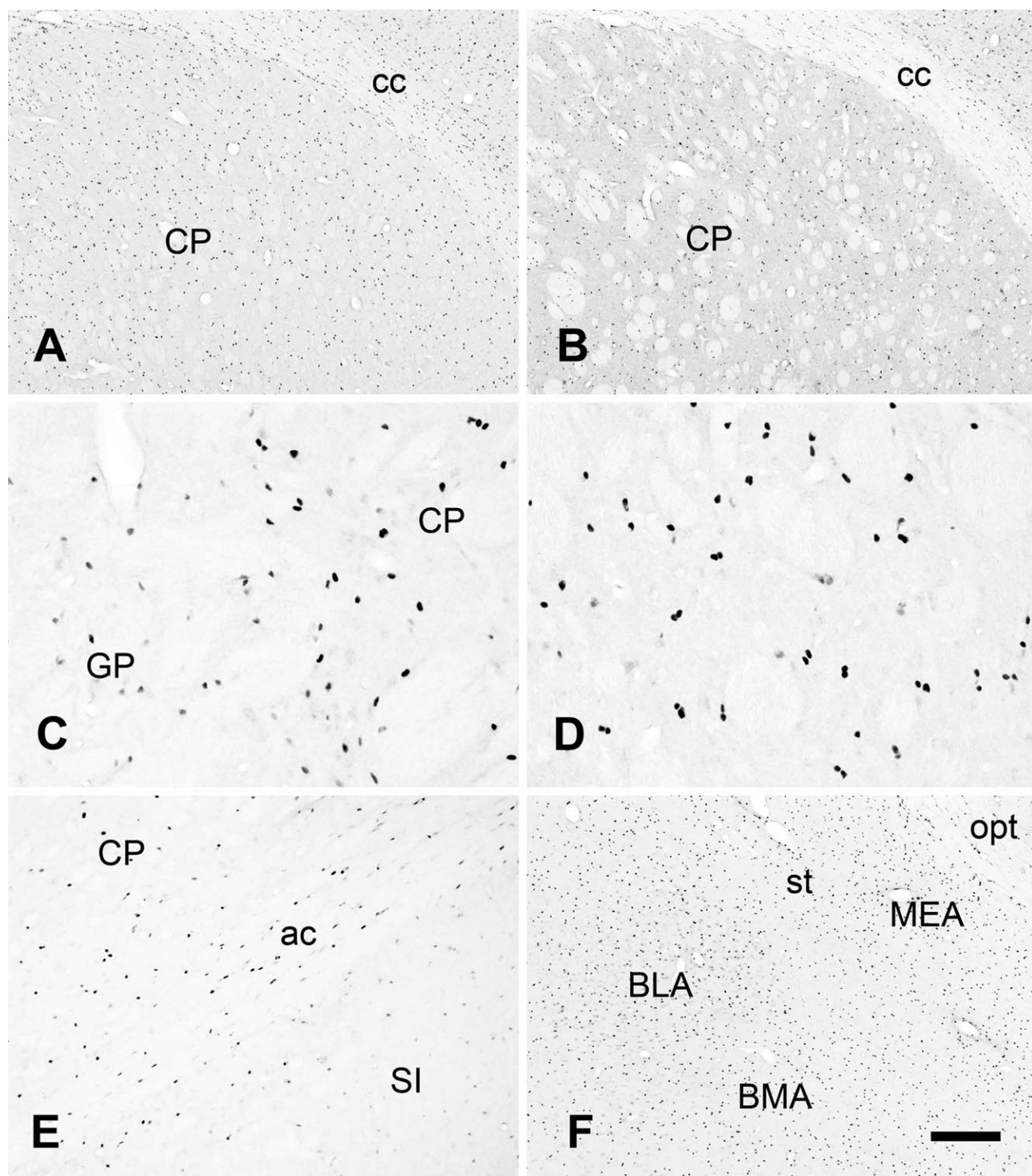


**Figure 11.** Telencephalic nuclei. Cell nuclei were immunoreactive throughout the dorsal striatum (caudate-putamen; CP) using both antibodies (A,B). Fewer immunoreactive cell nuclei were observed in the globus pallidus (GP) than in the caudate-putamen, and the stained nuclei in the globus pallidus were often less strongly immunoreactive than those in the caudate-putamen (C). As in neocortex, immunoreactive cell nuclei were often seen in closely associated pairs in the caudate-putamen (D). Structures immediately ventral to the anterior commissure (ac) such as the substantia innominata (SI) had relatively sparse AceCS1-IR (E). The amygdala contained many immunoreactive cell nuclei (F). ac, Anterior commissure; BLA, basolateral amygdalar nucleus; BMA, basomedial amygdalar nucleus; cc, corpus callosum; MEA, medial amygdalar nucleus; opt, optic chiasm; st, stria terminalis. A,C-F: protein antibody; B: affinity-purified peptide antibody. Scale bar = 300  $\mu$ m in F (applies to A,B,F); 60  $\mu$ m for C,D; 120  $\mu$ m for E.

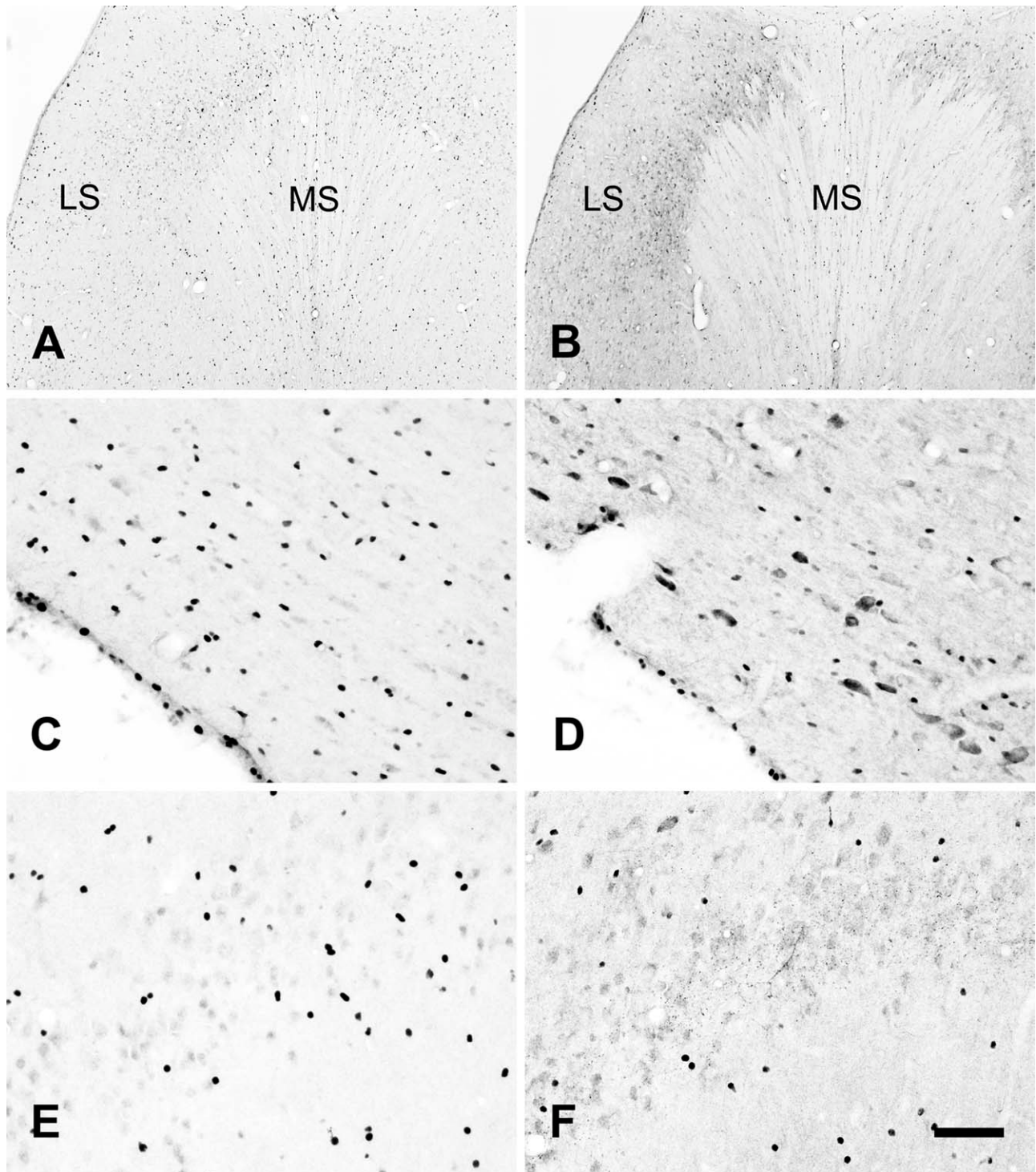


**Figure 12.** Septum, diagonal band, and piriform cortex. Immunoreactivity patterns with the protein (A) and peptide (B) antibodies were similar in the septum, except for greater neuronal staining with the antipeptide antibody (B). The same pattern was observed in the nucleus of the diagonal band, where the protein antibody stained predominantly cell nuclei (C), and the peptide antibody stained cell nuclei and a subpopulation of neurons (D). In piriform cortex, both antibodies stained cell nuclei (E,F), and the peptide antibody stained puncta on the surface of neurons as well (F). LS, lateral septum; MS, medial septum. A,C,E: protein antibody; B,D,F: affinity-purified peptide antibody. Scale bar = 60  $\mu\text{m}$  in F (applies to C-F); 300  $\mu\text{m}$  for A,B.

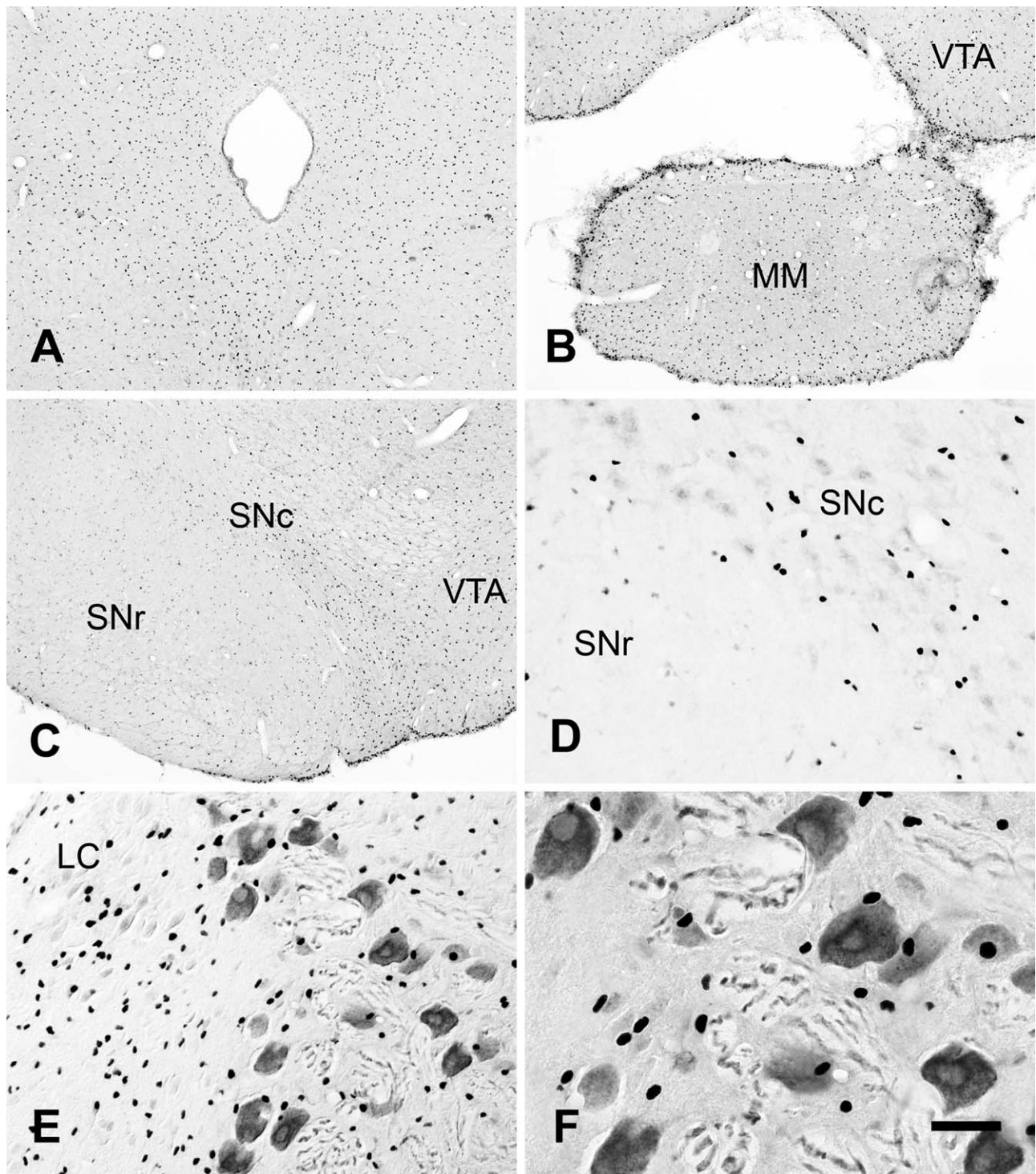


**Figure 13.** Midbrain. Numerous immunoreactive cell nuclei were present in the periaqueductal gray (A; PAG), ventral tegmental area (VTA), and medial mammillary nucleus (B; MM). The reticular portion of the substantia nigra (SNr) had relatively few immunoreactive cell nuclei, whereas a greater number of stained nuclei was present in the compact portion (SNc; C,D). The strongest neuronal staining in midbrain was observed in the mesencephalic trigeminal nucleus, where the large sensory neurons expressed AceCS1 in their cytoplasm, nuclei, and fibers (E,F). In some of these sensory neurons, expression was particularly strong at the periphery of the cell nuclei or in the perinuclear region (F). LC, locus coeruleus; MM, medial mammillary nucleus; SNc, substantia nigra compact region; SNr, substantia nigra reticular portion; VTA, ventral tegmental area. All images are from AceCS1 protein antibody-stained sections. Scale bar = 30  $\mu$ m in F; 300  $\mu$ m for A-C; 60  $\mu$ m for D,E.

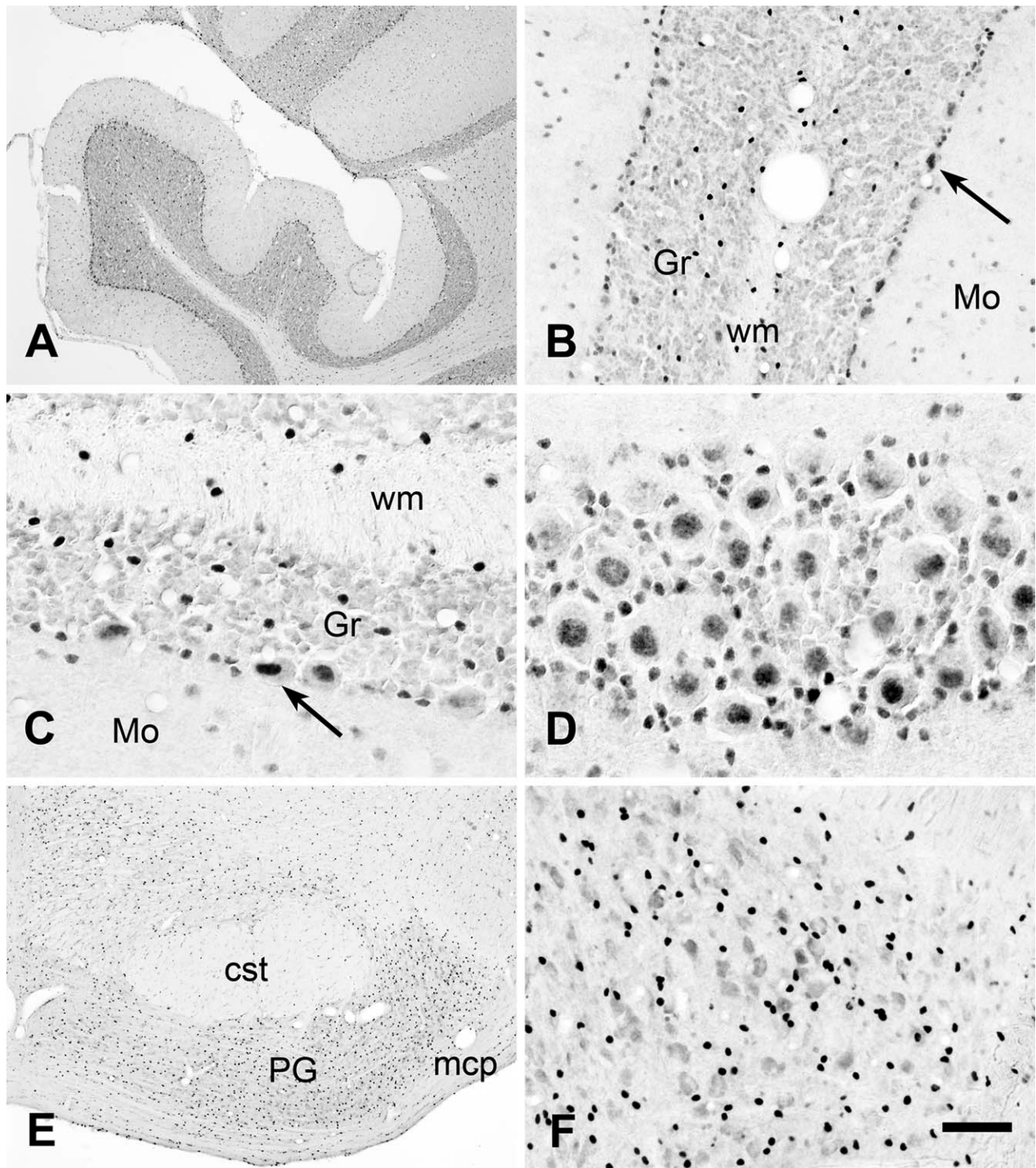


**Figure 14.** Cerebellum and pons. Low-magnification image of cerebellar cortex showing light to moderate immunoreactivity in all layers (A). Immunoreactive cell nuclei could be seen in the white matter (wm), granule cell (Gr), and molecular (Mo) layers (B,C). Purkinje cells ranged from unstained to moderately stained, and most immunoreactive Purkinje cells had stronger staining in their nuclei than in their cytoplasm (arrows in B,C). A slice through the Purkinje cell layer at high magnification shows the variability in nuclear AceCS1-IR (D). The pontine gray was notable for the high density of immunoreactive cell nuclei (E) as well as light to moderate immunoreactivity in many neurons (F). cst, Corticospinal tract; Gr, granule cell layer; mcp, middle cerebellar peduncle; Mo, molecular layer; PG, pontine gray; Wm, white matter. All images are from AceCS1 protein antibody-stained sections. Scale bar = 60  $\mu$ m in F (applies to C,F); 300  $\mu$ m for A,E; 120  $\mu$ m for B; 30  $\mu$ m for D.

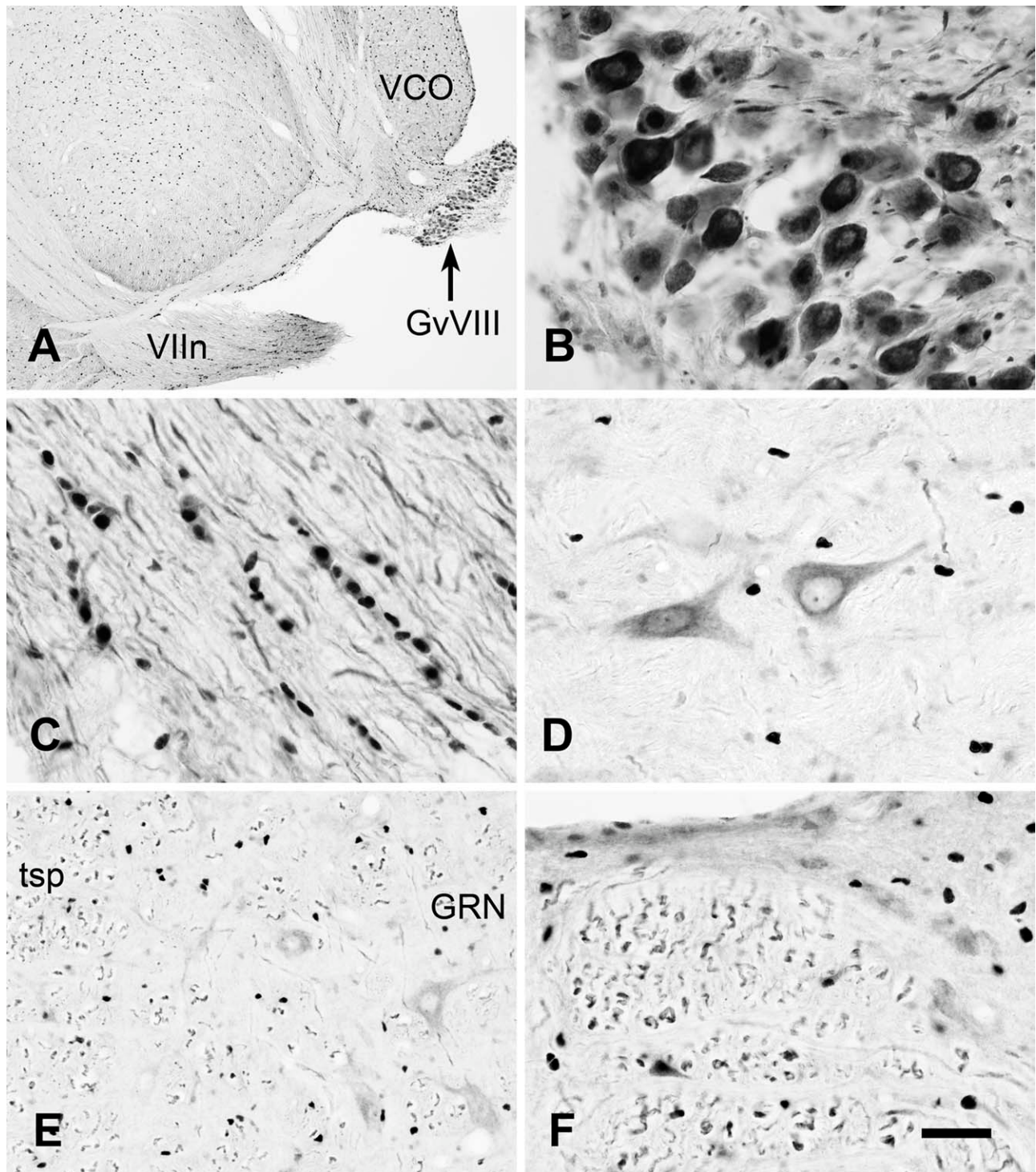


**Figure 15.** Brainstem. Similar to the sensory neurons in the mesencephalic trigeminal nucleus (see Fig. 13), the sensory ganglion cells of the vestibular ganglia (GvVIII) were moderately to strongly immunoreactive for AceCS1 (A,B). Immunoreactivity in these neurons was present in their cytoplasm, nuclei, and fibers and was variable between compartments. Some of these sensory ganglion cells had the highest levels of cytoplasmic staining observed in the brain (B). Oligodendrocytes were immunoreactive in their nuclei and cytoplasm in many brainstem fiber tracts and nerves, including the seventh nerve (VIIIn; A) and eighth nerve (C). Some large reticular neurons were lightly to moderately immunoreactive, typically with higher immunoreactivity in their cytoplasm than in their nuclei (D,E). Staining in some of these large neurons was particularly strong in the perinuclear region. Many axons throughout the brainstem were lightly to moderately immunoreactive for AceCS1, such as the fibers of the medial longitudinal fasciculus shown cut on end in F. All images are from AceCS1 protein antibody-stained sections. GRN, gigantocellular reticular nucleus; GvVIII, vestibular ganglion; tsp, tectospinal tract; VIIIn, seventh cranial nerve; VCO, ventral cochlear nucleus. Scale bar = 30  $\mu$ m in F (applies to B–D,F); 300  $\mu$ m for A; 60  $\mu$ m for E.

### AceCS1-IR in 18-day-old rat brain

AceCS1 expression was substantially stronger during brain postnatal development, with strong immunoreactivity in the cell nuclei of neurons and glial cells as well as increased cytoplasmic expression. Figure 16 shows AceCS1 expression in neocortex and fiber pathways in an 18-day-old rat. Cellular nuclei in all cortical layers were immunoreactive (Fig. 16A). Additionally, a much higher percentage of oligodendrocytes in white matter was immunoreactive in both the nuclei and the cytoplasm (Fig. 16B,C). In contrast with the adult brain, oligodendrocytes in 18-day-old rats were consistently stained in their cytoplasm (Fig. 16C,E). Also in contrast with adult rats, neuronal cell nuclei were much more consistently and strongly stained in 18-day-old developing rats (Fig. 16D). Some cellular nuclei in neuroepithelial areas where cell proliferation was taking place also expressed AceCS1 (Fig. 16F).

### AceCS1-IR in the injured rat brain

AceCS1 immunoreactivity was substantially up-regulated in the adult rat brain 3 days after unilateral CCI injury (Fig. 17). AceCS1 expression was substantially up-regulated in neurons after CCI injury (Fig. 17A,B), with the greatest increase in immunoreactivity occurring in neuronal cell nuclei. The up-regulation in AceCS1 expression was greatest in pyramidal cell nuclei in neocortex (Fig. 17C,D) and hippocampus (Fig. 17E,F). An increase in the number of immunoreactive nuclei in small nonneural cells was also observed in injured rat brains (compare Fig. 17A and B). In addition to the increased nuclear expression after injury, there was prominent immunoreactivity in brain capillaries that was not observed in uninjured brains (arrow in Fig. 17F).

## DISCUSSION

These initial studies on AceCS1 expression in the rat brain provide a few general conclusions but also raise many new questions. A major finding was that AceCS1 expression in the adult rat brain was not restricted to the cytoplasm of cells as expected (Fujino et al., 2001) but was present predominantly in the nuclei of cells. The yeast homolog of AceCS1 (designated *Acs2p* in yeast) was recently reported to be expressed in both cytoplasm and nuclei (Falcon et al., 2010) and was found to be involved in providing acetate for histone acetyltransferase reactions that regulate gene transcription (Takahashi et al., 2006). In several mammalian cell types in culture, AceCS1 was present in both the cytoplasm and the nucleus, with a predominant expression in cytoplasm (Wellen et al., 2009). Therefore, in eukaryotes, AceCS1 (AMP-forming type) is a nuclear-cytoplasmic enzyme

rather than a strictly cytosolic one. In the current study, we found that, in developing, adult, and injured rat brain, the predominant localization of AceCS1 was nuclear rather than cytoplasmic. Another generalization is that AceCS1 is expressed at higher levels during postnatal brain development than in the adult brain. This finding suggests that acetate metabolism through this pathway may be especially important during postnatal brain development, possibly by providing acetyl coenzyme A for histone acetylation reactions facilitating cellular differentiation and for lipid synthesis during postnatal myelination. Finally, the presence of AceCS1 in the cytoplasm of basal forebrain neurons, in puncta on the surface of cortical and hippocampal neurons, in the cell bodies of some brainstem neurons and ganglion cells, and in axons in many brainstem fiber pathways, could indicate that this enzyme is also involved in lipid synthesis or biochemical acetylation reactions requiring acetyl coenzyme A in the cytoplasmic compartment of some neurons.

The affinity-purified antipeptide antibodies used in these studies reacted with a protein doublet at approximately 76 kD on Western blots (Fig. 1), which is in good agreement with the published molecular weight of approximately 78 kD (Fujino et al., 2001). Immunoprecipitation of enzyme activity from solution and blocking of antibody binding to tissue sections with the antigen used for immunization indicated that the antipeptide antibodies are specific for AceCS1. Similarly, the antirecombinant AceCS1 antibodies reacted with an approximately 76-kD protein doublet, and immunoreactivity with this antibody was blocked by preincubation with the protein used for immunization. The polyclonal antisera against the recombinant AceCS1 protein provided generally stronger staining in cell nuclei, possibly because the antibodies were directed at multiple epitopes on the protein sequence. Both peptide and protein antibodies showed generally similar staining patterns in the brain, with some notable differences. The antipeptide AceCS1 antibodies stained substantially more neuronal cell bodies as well as staining small, punctate structures on the surface of neurons in specific brain areas. The antiprotein antibodies stained neuronal cytoplasm and puncta less but stained more cell nuclei and stained them more strongly than the antipeptide antibodies. These results suggest that the peptide and protein antibodies preferentially bound to the cytoplasmic and nuclear forms of AceCS1, respectively, perhaps as a result of increased accessibility of the N-terminus in the cytoplasmic form. Alternatively, because the 18-mer N-terminal sequence contains one lysine and four arginine residues, it is possible that it is a nuclear targeting sequence. If a portion of this sequence is cleaved after import of AceCS1 into the nucleus, then the antipeptide antibody, which was directed at the N-terminal sequence, would

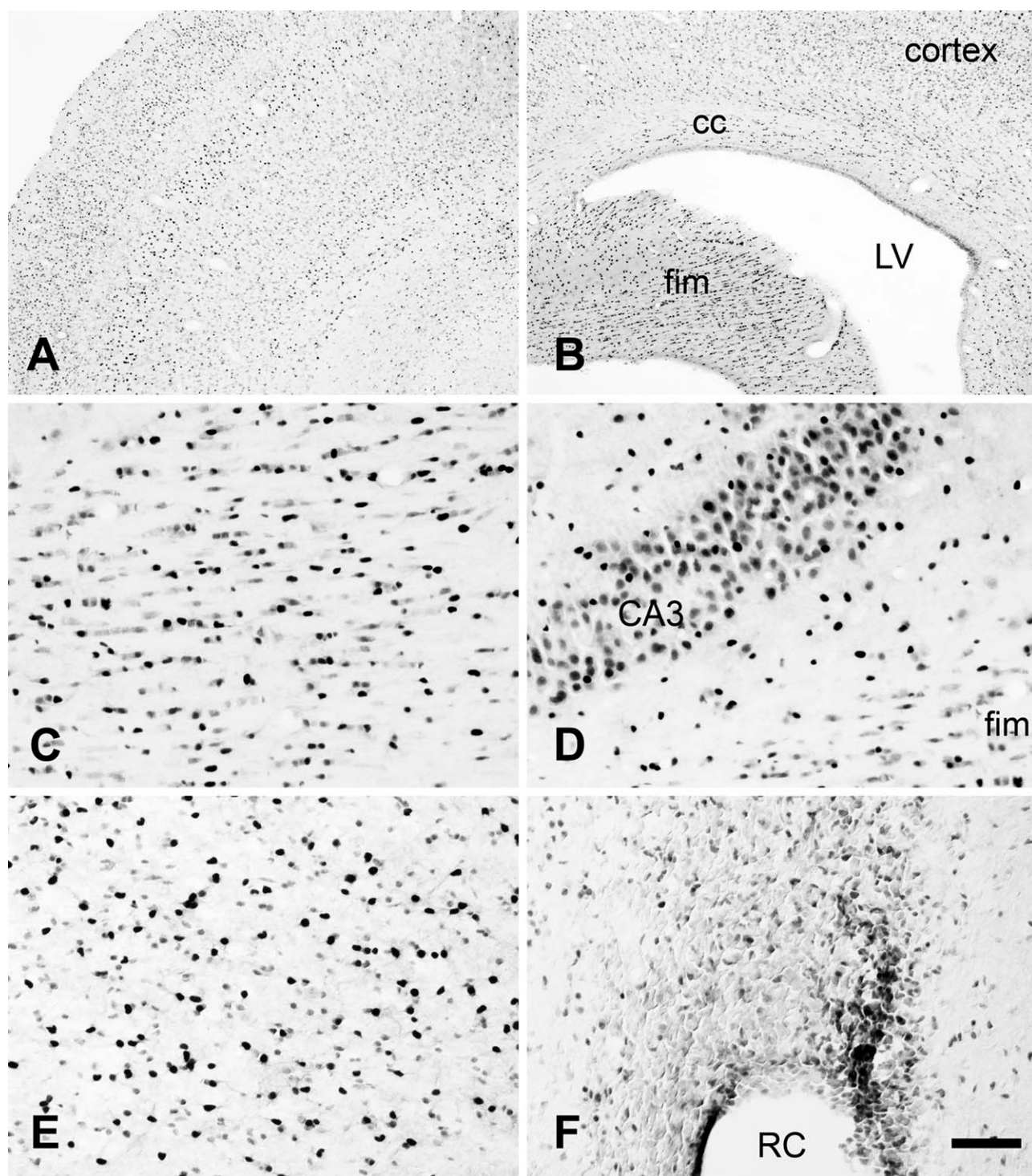


**Figure 16.** AceCS1 expression in 18-day-old rat brain. AceCS1 was expressed much more strongly in the brain during postnatal brain development, with numerous neurons in all cortical layers expressing AceCS1 (A). Oligodendrocytes were also strongly stained, including those in the corpus callosum (cc) and fimbria (fim; B,C). Most neurons were moderately to strongly immunoreactive, and expression was stronger in their nuclei than in their cytoplasm, for example, in the CA3 region of hippocampus (D). Oligodendrocytes were strongly stained at the anterior pole (forceps) of the corpus callosum (E). Moderate immunoreactivity was also seen in some neuroepithelial cells, such as those around the rhinocel (RC) in the frontal pole (F). All images are from AceCS1 recombinant protein antibody-stained sections. Scale bar = 60  $\mu\text{m}$  in F (applies to C-F); 300  $\mu\text{m}$  for A,B.

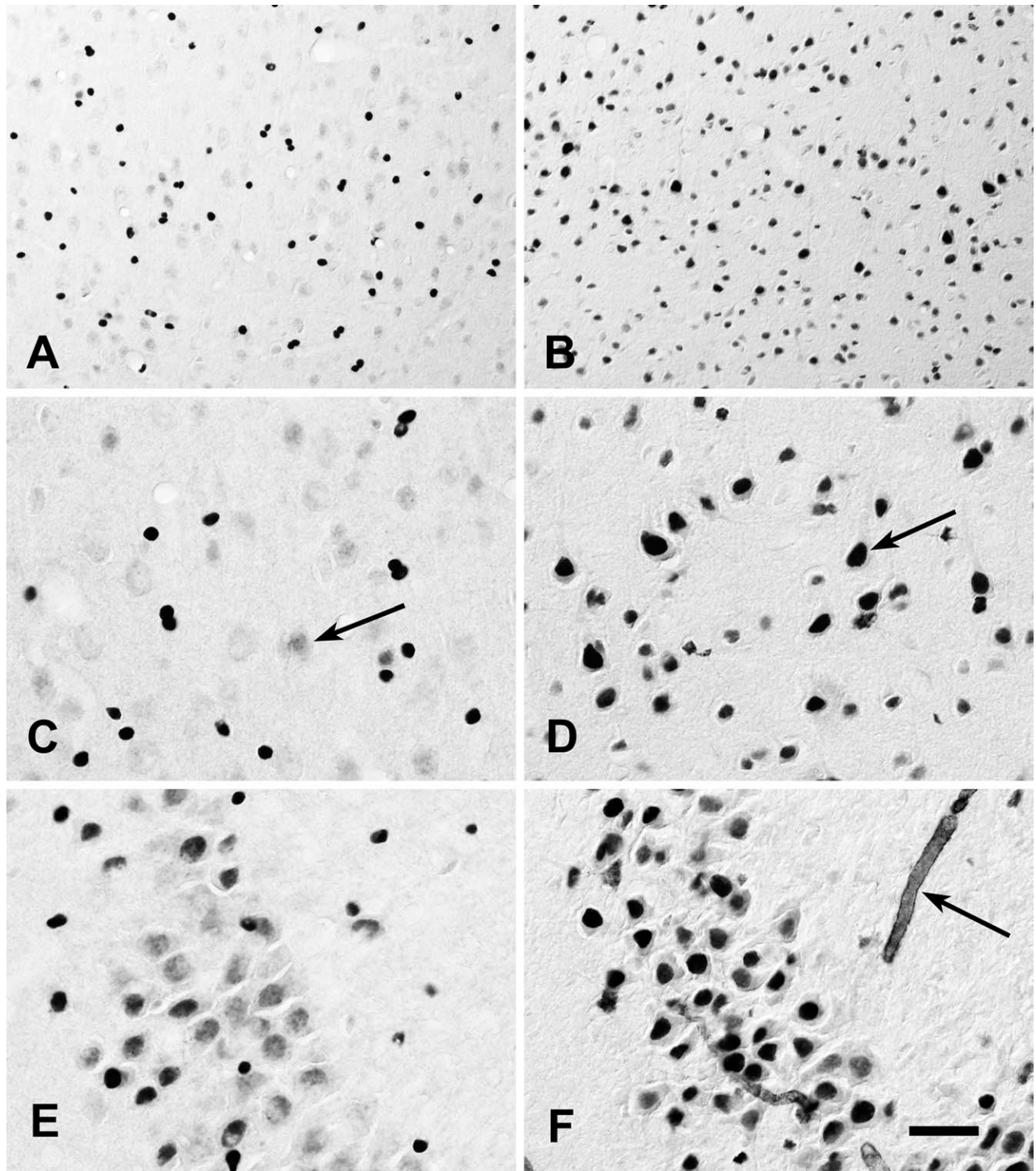


**Figure 17.** AceCS1-IR in the rat brain 3 days after experimental unilateral controlled cortical impact (CCI) injury. Neocortex in a control rat (A) is compared with the uninjured (contralateral) cortex in a rat 3 days after unilateral CCI injury (B). Strong up-regulation of AceCS1-IR occurred in neuronal cell nuclei, especially in larger pyramidal neurons. In uninjured rats, pyramidal cell nuclei were usually only very lightly immunoreactive (arrow in C), whereas, after injury, immunoreactivity was very strong in pyramidal cell nuclei (arrow in D). The same up-regulation of nuclear expression was observed in the hippocampus. For example, in uninjured adult rats, CA3 pyramidal neurons had light to moderate AceCS1-IR in their nuclei (E), but, in injured rats, expression in the nuclei of these neurons was strongly up-regulated (F). AceCS1-IR was also observed in capillaries after CCI injury (arrow in F). All images are from AceCS1 recombinant protein antibody-stained sections. DIC optics. Scale bar = 30  $\mu\text{m}$  in F (applies to C-F); 60  $\mu\text{m}$  for A,B.

react less strongly with the nuclear form of the enzyme, reducing nuclear immunoreactivity.

Unlike the case in mammalian cell lines studied in culture, which showed a predominantly cytoplasmic localization for AceCS1 (Wellen et al., 2009), immunoreactivity in the adult rat brain was predominantly nuclear in neurons, glia, ependymal cells, and endothelial cells. The low cytoplasmic expression of AceCS1 made cell identification difficult in many areas of the brain. Cytoplasmic staining was not observed in astrocytes or microglia, but the widespread distribution of immunoreactive cell nuclei in all parts of the brain suggests that AceCS1 was expressed intermittently in the nuclei of all cell types in the CNS. The observations of AceCS1 expression in the nuclei of CNS cells implicate this enzyme in acetylation reactions in chromatin, as has been shown for the homologous enzyme in yeast (Takahashi et al., 2006). It was found that the yeast mitochondrial and nuclear-cytoplasmic forms of AceCS were distinct and that the nuclear localized enzyme was involved in the regulation of chromatin activity via the action of histone acetyltransferases. AceCS1 expression was consistently stronger and more widespread in the brains of young rats still undergoing CNS development than in adults (Fig. 16). Unlike the case in adult brain, AceCS1 in 18-day-old brains was expressed in most neurons, with strong nuclear expression and light cytoplasmic expression, including proximal processes. Expression was also notably stronger in oligodendrocytes during the peak of postnatal myelination (18 days in rats) than it was in adult brains. The AceCS1 gene has been shown to be developmentally regulated, with strong expression in the developing brain (Loikkanen et al., 2002). Up-regulated expression in 18-day-old rat brains was observed predominantly in neuronal cell nuclei and the cytoplasm and nuclei of oligodendrocytes.

Furthermore, AceCS1 expression was found to be substantially up-regulated after brain injury, with the largest increase in immunoreactivity occurring in neurons, including cortical and hippocampal pyramidal neurons (Fig. 17). It is likely that the injury-associated increase in expression of AceCS1 in cell nuclei is associated with regions of chromatin where histone acetylation is active. Because AceCS1 utilizes free acetate to generate acetyl coenzyme A and is up-regulated after brain injury, we hypothesized that providing additional acetate in a form that could readily enter the brain would improve recovery after injury. We tested this hypothesis in the unilateral CCI model of brain injury in rats by administering the hydrophobic acetate precursor glyceryl-triacetate (GTA) to injured rats once per day and monitoring brain ATP and NAA levels and motor performance. We found that GTA administration significantly increased ATP and NAA levels in the injured hemisphere and increased the rate of motor

recovery compared with untreated injured rats (Arun et al., 2010). These findings provide support for the idea that GTA may be useful for treating brain injuries by providing acetate that can be used by AceCS1 and AceCS2 to boost cellular acetyl coenzyme A levels and facilitate recovery.

It is interesting to note that many of the cellular nuclei that were intensely stained for AceCS1 were observed in closely associated pairs throughout the brain, possibly suggesting that exceptionally strong nuclear AceCS1 expression is associated with global histone acetylation during glial and endothelial cell mitosis. Alternatively, because CC1-labeled oligodendrocytes with AceCS1-stained nuclei were also observed in closely associated pairs in areas such as the deeper layers of neocortex, it is possible that some of the paired nuclei with strong AceCS1 expression were from adjacent oligodendrocytes. For example, it has been reported that oligodendrocytes can be coupled to other oligodendrocytes by tight junctions (Massa and Mugnaini, 1982).

AceCS1 is an evolutionarily conserved enzyme that is critical for acetate metabolism across prokaryotes, plants, and animals (Ingram-Smith and Smith, 2007). It plays a central role in carbon metabolism in certain bacteria and therefore also in ruminants and other animals that harbor acetate-producing gut flora. The roles of AceCS1 in the mammalian brain remain speculative, insofar as little is known of its specific metabolic roles even in tissues in which it has been more extensively studied. AceCS1 transcription is regulated by sterol regulatory element-binding proteins (SREBP), and activity is negatively regulated by fasting, is increased upon refeeding, and contributes to lipid synthesis in some cell types (Sone et al., 2002). As an alternative pathway to the enzyme ATP citrate lyase, which converts citrate produced in mitochondria to acetyl coenzyme A in the cytosol, AceCS1 may be acting to provide an additional source of acetyl coenzyme A for the synthesis of fatty acids in the cytosol. There are several sources of free acetate in the mammalian brain; e.g., cytosolic acetyl coenzyme A hydrolase is one enzyme that can generate free acetate for lipid synthesis (Suematsu et al., 2002). AceCS1 could act to scavenge this acetate for resynthesis of acetyl coenzyme A (Luong et al., 2000). Histone deacetylases (HDACs) classes I and II may potentially produce substantial quantities of free acetate from histone and protein deacetylation both in the cytoplasm and in the nucleus. In the mammalian brain, N-acetylaspartate (NAA) has been shown to contribute free acetate for lipid synthesis in oligodendrocytes, but the enzyme responsible for converting NAA-derived acetate into usable acetyl coenzyme A remains to be identified (Moffett et al., 2007). The expression of AceCS1 in rat oligodendrocytes, especially during

postnatal myelination, implicates this enzyme in the activation of free acetate derived from NAA so that it can be used for metabolic or regulatory processes.

NAA is a molecule found at exceptionally high levels in the brain, with estimated concentrations between 8 and 11 mM (Bluml, 1999; Boumezbeur et al., 2009; Miyake et al., 1981; Tallan, 1957). NAA therefore represents one of the most concentrated metabolic sources of acetate in the human brain, yet the functions served by NAA remain elusive (for review see Moffett et al., 2007). NAA is synthesized in the cytoplasm and mitochondria of neurons (Ariyannur et al., 2008; Arun et al., 2009; Lu et al., 2004) via the enzyme aspartate N-acetyltransferase (Asp-NAT; Goldstein, 1969; Madhavarao et al., 2003). The enzyme Asp-NAT utilizes acetyl coenzyme A and aspartate to synthesize NAA, presumably when acetyl coenzyme A is in excess and requires conversion to a storage form of acetate. The enzyme aspartoacylase (ASPA), which is highly specific for NAA as a substrate (Kaul et al., 1991, 1993; Nambodiri et al., 2000), degrades NAA into free acetate and aspartate. ASPA is expressed strongly in oligodendrocytes in the CNS (Kirmani et al., 2002, 2003; Klugmann et al., 2003), where it has been shown to be a nuclear-cytoplasmic enzyme (Hershfield et al., 2006). ASPA is also expressed in microglia and to a more limited extent in some neurons and axons in the brainstem (Madhavarao et al., 2004). Together, Asp-NAT, NAA, ASPA, and AceCS1 represent a robust metabolic system for storing, transporting, and retrieving acetyl coenzyme A in the brain that can be utilized for diverse functions ranging from lipogenesis and protein acetylation in the cytoplasm to histone acetylation in cell nuclei.

AceCS1 was expressed in some oligodendrocytes in the adult rat brain, with stronger expression in nuclei than in cytoplasm. Many of the AceCS1-immunoreactive cell nuclei in the deeper layers of neocortex were also immunoreactive for the oligodendrocyte marker CC1 in their cytoplasm (see Fig. 5). We observed substantially stronger AceCS1 expression in oligodendrocytes in 18-day-old rats, during the period of postnatal myelination, including enhanced cytoplasmic expression. Therefore, both AceCS1 and ASPA are expressed in oligodendrocytes during myelination, implicating AceCS1 in the production of acetyl coenzyme A from NAA-derived acetate for the purpose of myelin lipid synthesis and gene regulation during oligodendrocyte maturation. Genetic mutations in the gene encoding ASPA result in a fatal dysmyelinating disorder known as *Canavan disease*. Because NAA is one of the most concentrated sources of acetate in the brain, the inability to deacetylate NAA in Canavan disease results in an approximately 80% reduction in brain acetate levels during postnatal myelination (Madhavarao et al., 2005). It is likely that this reduced acetate availabil-

ity during postnatal brain development would have deleterious effects on myelin lipid synthesis, and histone acetylation reactions required for cell differentiation.

The expression of AceCS1 in puncta on the surface of neurons in hippocampus and cortex, in neurons of the basal forebrain, and in neurons and axons in the brainstem, including relatively strong immunoreactivity in primary sensory neurons, raises the possibility that this enzyme might play some limited role in the synthesis of acetylcholine (Baurle et al., 1999). Reports have suggested that at least some of the acetyl coenzyme A used for acetylcholine synthesis is made from free acetate via AceCS1 rather than via the ATP citrate lyase pathway (Benjamin and Quastel, 1981). However, free acetate is not the primary source of acetyl coenzyme A for acetylcholine synthesis (Kwok and Collier, 1982). Citrate is the primary substrate for acetyl coenzyme A synthesis and, therefore, the primary source of substrate for acetylcholine synthesis. In addition to citrate, free acetate generated from acetylcholine by the action of cholinesterase can be taken up and reused for the synthesis of acetylcholine (Carroll, 1997), as is the case with choline. Additional research will be required to determine what role AceCS1 plays in recycling acetate derived from acetylcholine breakdown.

It has been noted that metabolic enzymes such as AceCS1 do not typically participate directly in gene regulation, but the nucleocytoplasmic form of AceCS in yeast has been shown to be involved in histone acetylation and regulation of global gene transcription (Takahashi et al., 2006). This raises the possibility that AceCS1, which we have shown to be a nuclear-cytoplasmic enzyme in the rat CNS, serves a similar function in the mammalian brain. In vitro studies of mammalian cell lines comparing the relative contributions of AceCS1 and citrate lyase to histone acetylation showed that citrate lyase is the predominant source of acetate for these reactions (Wellen et al., 2009). The mammalian cell lines investigated included HCT116 human colon carcinoma cells, LN229 human glioblastoma cells, and immortalized mouse embryo fibroblasts. In these cells in culture, the citrate lyase contribution to histone acetylation was significantly more robust than that from AceCS1. Furthermore, Wellen et al. found a predominant cytoplasmic localization of AceCS1, which was in contrast to the results we obtained in the mammalian brain. For the rat brain, we found that AceCS1 was expressed most strongly in cell nuclei rather than in the cytoplasm. Expression was variable in the nuclei of neurons and glial cells, and expression was stronger during postnatal brain development, and after brain injury, than in uninjured adult brains. Based on its distribution in different cell types and the presence in both cell nuclei and cytoplasm, these localization studies provide further evidence that AceCS1 is a multifunctional enzyme in

mammals. AceCS1 represents an alternative source of acetyl coenzyme A to the citrate lyase pathway and provides some of the acetate for nuclear acetylation reactions as well as some of the acetate required for cytoplasmic lipid synthesis in the brain. It is likely that AceCS1 supplies acetyl coenzyme A for other acetylation reactions as well, including endoplasmic reticulum protein acetylation required for maintaining proper protein conformation during synthesis. One possibility worthy of investigation is that the AceCS1 pathway is more critical for acetyl coenzyme A production in the CNS under ketogenic conditions, when glucose availability is low. These findings offer challenging tasks for researchers to determine the functional significance of AceCS1 expression in the nuclei of neurons and glial cells, the sources of free acetate that this enzyme uses to synthesize acetyl coenzyme A in different cell types, and the regulatory mechanisms that control its expression during development and in response to injury.

## LITERATURE CITED

- Ariyannur PS, Madhavarao CN, Namboodiri AM. 2008. N-acetylaspartate synthesis in the brain: mitochondria vs. microsomes. *Brain Res* 1227:34–41.
- Arun P, Moffett JR, Namboodiri AM. 2009. Evidence for mitochondrial and cytoplasmic N-acetylaspartate synthesis in SH-SY5Y neuroblastoma cells. *Neurochem Int* 55:219–225.
- Arun P, Ariyannur PS, Moffett JR, Xing G, Hamilton K, Grunberg NE, Ives JA, Namboodiri AM. 2010. Metabolic acetate therapy for the treatment of traumatic brain injury. *J Neurotrauma* 27:293–298.
- Baurle J, Bruning G, Schemann M, Nishiike S, Guldin WO. 1999. Co-localization of glutamate, choline acetyltransferase and glycine in the mammalian vestibular ganglion and periphery. *Neuroreport* 10:3517–3521.
- Benjamin AM, Quastel JH. 1981. Acetylcholine synthesis in synaptosomes: mode of transfer of mitochondrial acetyl coenzyme A. *Science* 213:1495–1497.
- Bluml S. 1999. In vivo quantitation of cerebral metabolite concentrations using natural abundance  $^{13}\text{C}$  MRS at 1.5 T. *J Magn Reson* 136:219–225.
- Boumezbear F, Mason GF, de Graaf RA, Behar KL, Cline GW, Shulman GI, Rothman DL, Petersen KF. 2009. Altered brain mitochondrial metabolism in healthy aging as assessed by in vivo magnetic resonance spectroscopy. *J Cereb Blood Flow Metab* 30:211–221.
- Carroll PT. 1997. Evidence to suggest that extracellular acetate is accumulated by rat hippocampal cholinergic nerve terminals for acetylcholine formation and release. *Brain Res* 753:47–55.
- Falcon AA, Chen S, Wood MS, Aris JP. 2010. Acetyl-coenzyme A synthetase 2 is a nuclear protein required for replicative longevity in *Saccharomyces cerevisiae*. *Mol Cell Biochem* 333:99–108.
- Fujino T, Kondo J, Ishikawa M, Morikawa K, Yamamoto TT. 2001. Acetyl-CoA synthetase 2, a mitochondrial matrix enzyme involved in the oxidation of acetate. *J Biol Chem* 276:11420–11426.
- Goldberg RP, Brunengraber H. 1980. Contributions of cytosolic and mitochondrial acetyl-CoA syntheses to the activation of lipogenic acetate in rat liver. *Adv Exp Med Biol* 132:413–418.
- Goldstein FB. 1969. The enzymatic synthesis of N-acetyl-L-aspartic acid by subcellular preparations of rat brain. *J Biol Chem* 244:4257–4260.
- Hallows WC, Lee S, Denu JM. 2006. Sirtuins deacetylate and activate mammalian acetyl-CoA synthetases. *Proc Natl Acad Sci U S A* 103:10230–10235.
- Hershfield J, Madhavarao CN, Moffett JR, Benjamins JA, Garbern JY, Namboodiri MA. 2006. Aspartoacylase is a regulated nuclear-cytoplasmic enzyme. *FASEB J* 20:2139–2141.
- Imesch E, Rous S. 1984. Partial purification of rat liver cytoplasmic acetyl-CoA synthetase; characterization of some properties. *Int J Biochem* 16:875–881.
- Ingram-Smith C, Smith KS. 2007. AMP-forming acetyl-CoA synthetases in Archaea show unexpected diversity in substrate utilization. *Archaea* 2:95–107.
- Kaul R, Casanova J, Johnson AB, Tang P, Matalon R. 1991. Purification, characterization, and localization of aspartoacylase from bovine brain. *J Neurochem* 56:129–135.
- Kaul R, Gao GP, Balamurugan K, Matalon R. 1993. Cloning of the human aspartoacylase cDNA and a common missense mutation in Canavan disease. *Nat Genet* 5:118–123.
- Kirmani BF, Jacobowitz DM, Kallarakal AT, Namboodiri MA. 2002. Aspartoacylase is restricted primarily to myelin synthesizing cells in the CNS: therapeutic implications for Canavan disease. *Brain Res Mol Brain Res* 107:176–182.
- Kirmani BF, Jacobowitz DM, Namboodiri MA. 2003. Developmental increase of aspartoacylase in oligodendrocytes parallels CNS myelination. *Brain Res Dev Brain Res* 140:105–115.
- Klugmann M, Symes CW, Klausner BK, Leichtlein CB, Serikawa T, Young D, Doring MJ. 2003. Identification and distribution of aspartoacylase in the postnatal rat brain. *Neuroreport* 14:1837–1840.
- Kornacker MS, Lowenstein JM. 1965. Citrate and the conversion of carbohydrate into fat. The activities of citrate-cleavage enzyme and acetate thiokinase in livers of starved and re-fed rats. *Biochem J* 94:209–215.
- Kuang Y, Salem N, Wang F, Schomisch SJ, Chandramouli V, Lee Z. 2007. A colorimetric assay method to measure acetyl-CoA synthetase activity: application to woodchuck model of hepatitis virus-induced hepatocellular carcinoma. *J Biochem Biophys Methods* 70:649–655.
- Kwok YN, Collier B. 1982. Synthesis of acetylcholine from acetate in a sympathetic ganglion. *J Neurochem* 39:16–26.
- Loikkanen I, Haghighi S, Vainio S, Pajunen A. 2002. Expression of cytosolic acetyl-CoA synthetase gene is developmentally regulated. *Mech Dev* 115:139–141.
- Lu ZH, Chakraborty G, Ledeen RW, Yahya D, Wu G. 2004. N-acetylaspartate synthase is bimodally expressed in microsomes and mitochondria of brain. *Brain Res Mol Brain Res* 122:71–78.
- Luong A, Hannah VC, Brown MS, Goldstein JL. 2000. Molecular characterization of human acetyl-CoA synthetase, an enzyme regulated by sterol regulatory element-binding proteins. *J Biol Chem* 275:26458–26466.
- Madhavarao CN, Chinopoulos C, Chandrasekaran K, Namboodiri MA. 2003. Characterization of the N-acetylaspartate biosynthetic enzyme from rat brain. *J Neurochem* 86:824–835.
- Madhavarao CN, Moffett JR, Moore RA, Viola RE, Namboodiri MA, Jacobowitz DM. 2004. Immunohistochemical localization of aspartoacylase in the rat central nervous system. *J Comp Neurol* 472:318–329.
- Madhavarao CN, Arun P, Moffett JR, Szucs S, Surendran S, Matalon R, Garbern J, Hristova D, Johnson A, Jiang W, Namboodiri MA. 2005. Defective N-acetylaspartate catabolism reduces brain acetate levels and myelin lipid synthesis in Canavan's disease. *Proc Natl Acad Sci U S A* 102:5221–5226.

- Massa PT, Mugnaini E. 1982. Cell junctions and intramembrane particles of astrocytes and oligodendrocytes: a freeze-fracture study. *Neuroscience* 7:523–538.
- Miyake M, Kakimoto Y, Sorimachi M. 1981. A gas chromatographic method for the determination of N-acetyl-L-aspartic acid, N-acetyl-aspartylglutamic acid and beta-citryl-L-glutamic acid and their distributions in the brain and other organs of various species of animals. *J Neurochem* 36:804–810.
- Moffett JR, Ross B, Arun P, Madhavarao CN, Namboodiri AM. 2007. N-acetylaspartate in the CNS: from neurodiagnostics to neurobiology. *Prog Neurobiol* 81:89–131.
- Namboodiri MA, Corigliano-Murphy A, Jiang G, Rollag M, Provensio I. 2000. Murine aspartoacylase: cloning, expression and comparison with the human enzyme. *Brain Res Mol Brain Res* 77:285–289.
- Papay R, Gaivin R, Jha A, McCune DF, McGrath JC, Rodrigo MC, Simpson PC, Doze VA, Perez DM. 2006. Localization of the mouse alpha1A-adrenergic receptor (AR) in the brain: alpha1AAR is expressed in neurons, GABAergic interneurons, and NG2 oligodendrocyte progenitors. *J Comp Neurol* 497:209–222.
- Pow DV, Crook DK. 1993. Extremely high titre polyclonal antisera against small neurotransmitter molecules: rapid production, characterisation and use in light- and electron-microscopic immunocytochemistry. *J Neurosci Methods* 48:51–63.
- Sakakibara I, Fujino T, Ishii M, Tanaka T, Shimosawa T, Miura S, Zhang W, Tokutake Y, Yamamoto J, Awano M, Iwasaki S, Motoike T, Okamura M, Inagaki T, Kita K, Ezaki O, Naito M, Kuwaki T, Chohnan S, Yamamoto TT, Hammer RE, Kodama T, Yanagisawa M, Sakai J. 2009. Fasting-induced hypothermia and reduced energy production in mice lacking acetyl-CoA synthetase 2. *Cell Metab* 9:191–202.
- Schwer B, Verdin E. 2008. Conserved metabolic regulatory functions of sirtuins. *Cell Metab* 7:104–112.
- Skutches CL, Holroyde CP, Myers RN, Paul P, Reichard GA. 1979. Plasma acetate turnover and oxidation. *J Clin Invest* 64:708–713.
- Sone H, Shimano H, Sakakura Y, Inoue N, Amemiya-Kudo M, Yahagi N, Osawa M, Suzuki H, Yokoo T, Takahashi A, Iida K, Toyoshima H, Iwama A, Yamada N. 2002. Acetyl-coenzyme A synthetase is a lipogenic enzyme controlled by SREBP-1 and energy status. *Am J Physiol Endocrinol Metab* 282:E222–E230.
- Spange S, Wagner T, Heinzel T, Kramer OH. 2009. Acetylation of nonhistone proteins modulates cellular signalling at multiple levels. *Int J Biochem Cell Biol* 41:185–198.
- Starai VJ, Celic I, Cole RN, Boeke JD, Escalante-Semerena JC. 2002. Sir2-dependent activation of acetyl-CoA synthetase by deacetylation of active lysine. *Science* 298:2390–2392.
- Suematsu N, Okamoto K, Isohashi F. 2002. Mouse cytosolic acetyl-CoA hydrolase, a novel candidate for a key enzyme involved in fat metabolism: cDNA cloning, sequencing and functional expression. *Acta Biochim Pol* 49:937–945.
- Szutowicz A, Lysiak W. 1980. Regional and subcellular distribution of ATP-citrate lyase and other enzymes of acetyl-CoA metabolism in rat brain. *J Neurochem* 35:775–785.
- Takahashi H, McCaffery JM, Irizarry RA, Boeke JD. 2006. Nucleocytosolic acetyl-coenzyme a synthetase is required for histone acetylation and global transcription. *Mol Cell* 23:207–217.
- Tallan HH. 1957. Studies on the distribution of N-acetyl-L-aspartic acid in brain. *J Biol Chem* 224:41–45.
- Wellen KE, Hatzivassiliou G, Sachdeva UM, Bui TV, Cross JR, Thompson CB. 2009. ATP-citrate lyase links cellular metabolism to histone acetylation. *Science* 324:1076–1080.
- Woodnutt G, Parker DS. 1978. Rabbit liver acetyl-CoA synthetase. *Biochem J* 175:757–759.